International Climate News

M. J. Arteaga-Garavito R. Colacito M. M. Croce B. Yang*

Abstract

We develop novel high-frequency indices that measure climate attention across a wide range of developed and emerging economies. By analyzing the text of over 23 million Tweets published by leading national newspapers, we find that a country experiencing more severe climate news shocks tends to see both an inflow of capital and an appreciation of its currency. In addition, brown stocks experience large and persistent negative returns after a global climate news shock if located in highly exposed countries. A risk-sharing model in which investors price climate news shocks and trade consumption and investment goods in global markets rationalizes these findings.

First Draft: June 28, 2023. This Draft: June 30, 2025.
Keywords: International Climate Indices, Text Analysis, Trade, Currencies.
JEL Classification: F3, F4, G1.

*Maria Jose Arteaga-Garavito is a PhD Student at Bocconi University (email: majo_arteaga@hotmail.com; Twitter: @MajoArteaga). Riccardo Colacito is affiliated with the Kenan-Flagler Business School at UNC Chapel Hill and NBER (email: ric@unc.edu; Twitter: @RColacito). Mariano Massimiliano Croce is affiliated with Bocconi University, CEPR, IGIER and Baffi-Carefin (email: mmc287@gmail.com; Twitter: @MCroce_MacroFin); Biao Yang is affiliated to the Shanghai Jiao Tong University (biao.yang@sjtu.edu.cn; Twitter: @Biao90). We thank Elena Carletti, Anna Pavlova, Lars Hansen, Monika Piazzesi and Marcin Kacperczyk for useful feedback on the paper, as well as our discussant Zhengyang Jiang, Juri Marcucci, Zhe Geng, Jinfei Sheng, Yasmine Van der Straten, Cristina Angelico, and Alminas Žaldokas. We also thank seminar participants at the NBER SI IFM meeting, the EFA, the LUISS Finance conference, the SED, the Econometrics Society Meetings (Asia), ECONDAT Banca d'Italia, the European Commission, the CFRN Young Finance Scholars Meeting, the CICF, the Workshop on AI in Finance and Digital Economy at HKUST (Guangzhou), the International Finance Society Conference, Boston University, University of Virginia, Shanghai Jiao Tong University, and Peking University.

1 Introduction

In recent years, there has been a growing focus on the interaction between climate dynamics and economic activities. Predicted changes in climate patterns are expected to result in a significant redistribution of economic operations across various locations, sectors, and corporations. At the same time, the valuation of stocks and bonds is increasingly reflecting climate risk factors. However, to the best of our knowledge, there has been limited attention given to the relationship between climate-related news shocks and international economic variables, such as currencies and global capital flows.

In this paper, we develop a new international general equilibrium model with climate news shocks to generate testable predictions for asset prices, exchange rates, and international trade. To empirically test the model, we construct a new index that captures high-frequency climate news shocks based on the content of Twitter feeds from major newspapers in both advanced and emerging economies. By adopting a high-frequency approach, we mitigate the challenges of studying the long-run effects of climate shocks in short samples and offer new insights for asset pricing.

We document three main empirical findings. First, countries with greater exposure to climate news shocks experience a persistent currency appreciation. Second, brown firms located in highly exposed countries tend to experience large negative and persistent stock returns after adverse climate news shocks. To the best of our knowledge, we are the first to document no significant effect on high-emission firms located in countries with low exposure to climate news shocks. Third, international current accounts respond to climate news shocks in a manner consistent with a recursive risk-sharing mechanism. Specifically, countries that are highly sensitive to climate news shocks hedge through international financial markets and receive resources—reflected in a decline in net exports—when adverse news shocks materialize. This result highlights the significant impact of climate news on both international asset prices and economic variables.

On the theory side, we consider a general equilibrium model in which: (i) investors price climate news shocks (Colacito et al. 2018); (ii) investment goods can be used to increase either green or brown assets; (iii) there are both productivity and global climate news shocks; and (iv) countries have different sensitivities toward climate

news (denoted as b).

To derive analytical expressions, we focus on a two-country, two-period model in which time-1 utility depends on both consumption and a sentiment component linked to global climate news shocks, mediated by the sensitivity parameter b. At time 2, production is endogenous and determined by investment decisions made at time 1. Time-2 utility is influenced by exogenous productivity shocks as well as disruptions caused by brown assets, which can be partially offset by green assets. Importantly, "disruption" is interpreted broadly to include both potential physical damages and transition risks. We assume complete markets, allowing the two countries to trade time-0 securities to hedge against both productivity and climate sentiment shocks. To the best of our knowledge, this is the first general equilibrium model in the climate finance literature to incorporate priced climate news in a multi-country setting. While the model is intentionally stylized to highlight the core mechanism, it offers a valuable and tractable framework for understanding the role of these risks in an international context.

Specifically, our model predicts that a country more sensitive to a global climate news shock (i.e., with higher b) should experience both a currency appreciation and a decline in net exports when an adverse climate news shock materializes. A decline in net exports corresponds to an inflow of resources—consistent with the transfer prescribed by international risk-sharing. In addition, the model allows us to study the returns on both brown and green assets. An investment strategy that is long brown assets and short green assets delivers a negative excess return following an adverse global climate news shock. This loss is more pronounced in countries with greater sensitivity to climate news.

To test the predictions of our model, we apply textual analysis techniques to the full universe of tweets posted by major national newspapers across 25 countries between 2014 and 2022. We compute a cosine-similarity score with a climate-related reference corpus and use these scores to build a daily climate-attention measure for each country. These indices contain a common component, which we denote as the global climate attention index. Importantly, there is substantial heterogeneity in the country-level loadings on this global component. We denote these loadings as βs and interpret them as the empirical counterpart to the sensitivity of country-level sentiment to global climate news shocks—that is, the model's b coefficient. In both the data

and the model, this dimension of cross-country heterogeneity is distinct from existing measures of climate vulnerability.

We identify days of high attention toward climate news and study the behavior of currencies after these days. We find that after negative climate-related news, the currencies of high-β countries appreciate. This result adds empirical support to the theoretical link between climate news shocks and currency values.

Additionally, in line with the empirical asset pricing literature, we estimate sensitivity coefficients of returns over various horizons and for more than 17,000 firms. We examine firms with varying emission intensities located in all the countries included in our study. Importantly, in our empirical investigation we use an interaction term comprising emissions and country-level exposure. The literature has already documented that climate attention shocks are followed by negative cumulative stock returns. We find that this effect is highly persistent and is concentrated among brown firms that are located in countries with high exposure. In contrast, brown firms in countries with low exposure exhibit no significant response in their equity returns.

Our climate attention indicators can be aggregated to the quarterly level, enabling us to combine them with lower-frequency international trade data. We find empirical support for the third prediction of our model—namely, that countries more exposed to climate news shocks receive resources through lower net exports.

In what follows, we provide a more detailed description of the novel contribution related to our climate news index. More specifically, as in Engle et al. (2020), we construct a climate attention index that measures the extent to which climate change is discussed in the news media. However, our method differs in that we focus on newspapers with a significant presence on Twitter across many countries. This approach allows us to compile a large dataset of over 23 million tweets, which we then aggregate at the country level across daily, weekly, monthly, and quarterly frequencies. We compare the aggregated text to a corpus of authoritative texts on climate change, similar to the method used by Engle et al. (2020). As of the date of this draft, our data coverage refers to a total of 25 countries that span a wide range of local languages, income levels, and geographical regions.

We construct climate news indices at the country level and aggregate them to create a global index by computing cross-country averages weighted equally, by GDP, and

by Twitter volume (data available on our website). For each country in our dataset, we regress its country-specific climate index on the global index. The estimated slope, denoted as β, measures each country's exposure to common or, equivalently, global news. Across countries, we find a substantial degree of variation in exposure. Importantly, our measure of sensitivity is weakly correlated with both the vulnerability score provided by the Notre Dame Global Adaptation Initiative and absolute latitude, implying that we are focusing on a distinct dimension of heterogeneity that is not directly related to vulnerability and that we interpret as climate-related sentiment.

Leveraging our granular dataset, we use high-frequency data to identify the impact of climate news shocks on asset prices. Specifically, we analyze the reaction of currencies and stocks in the days following a substantial increase in climate attention. To achieve this, we compute daily innovations in our global climate index and focus on the top 15% of these observations. This approach allows us to (i) reduce noise from non-climate-related news and (ii) better isolate days driven by "pure" climate news shocks. Such a methodology is commonly employed in the literature on identifying the effects of news related to policy announcements (Leombroni et al. 2021). Importantly, some days with substantial climate-related news might fall below the top 15% threshold due to the prominence of other topics in the news. Consequently, as is typical in this literature, we may have a downward bias, i.e., a reduced likelihood of detecting a significant effect of climate news on asset prices and currencies.

We further incorporate a sentiment analysis of climate-related tweets on days with high climate attention. Using the BERTopic algorithm, we cluster all tweets into topics and identify those closely related to climate. This subset is then divided into two groups based on whether the topic primarily pertains to climate-related physical or transition risk. Following this classification, each tweet on a given day is categorized as related to physical risk, transition risk, or non-climate topics. We apply multilingual sentiment classifiers to distinguish between positive and negative content. Our findings indicate that days with extremely high climate attention are predominantly characterized by negative climate-related news. The reaction of currencies and stock returns is mainly driven by negative news about transition risk.

Our analysis using daily-frequency data reveals that currencies of countries with higher exposure to our global climate index tend to appreciate following climate news shocks, with this effect persisting over several days. Remarkably, this finding is ob-

served not only in pairs of advanced economies but also in combinations involving at least one developing country. Moreover, the robustness of this finding is upheld regardless of (i) the method used for aggregating country-level climate indices into a single global index, and (ii) whether we use weekly or daily data.

Related literature. An important strand of recent literature employs textual analysis of earnings conference call transcripts to assess exposure to climate risk (see, for example, Sautner et al. 2023, Hassan et al. 2019 and Hassan et al. 2023). We differ from this literature in that we focus on the public interest for climate, rather than on educated firm-level experts. Moreover, our access to social media outlets allows us to construct a high-frequency index for a large cross-section of countries.

Our frictionless model builds on the tradition of international macro-finance models with recursive preferences and news shocks (Colacito et al. 2018). We present a unified framework to document that currencies, international capital flows, and investments in brown and green technologies are related to our climate-related news. We leave the study of settings with segmented markets (see, among others, Sandulescu et al. 2020) to future work.

A substantial body of literature has examined the behavior, predictability, and volatility of exchange rates (Della Corte et al. 2009; Della Corte et al. 2011; Della Corte et al. 2016). Our analysis contributes to this stream by focusing on the dynamic response of the foreign exchange market to news. In international asset pricing, extensive research has developed and analyzed models to understand asset prices, exchange rates, and macroeconomic interactions across countries (Pavlova and Rigobon 2007, 2010, 2013; Hassan 2013; Hassan et al. 2015, 2016; Zviadadze 2017). We contribute to the broader understanding of international macroeconomic dynamics and asset valuation in response to global climate-related events.

Another line of research investigates the impact of political and economic risk on firms, asset markets, and international economic linkages (Hassan et al. 2019, 2023). This literature develops methodologies to quantify various risks and uncertainties and assesses their economic and financial spillovers. Our study introduces a novel text-based measure of global attention to climate change as an indicator of perceived risk and uncertainty. Furthermore, we document the influence of our index on cur-

rency markets and international financial dynamics.

The literature on carry trade strategies has linked their risk premia to global risk factors (see, for example, Lustig et al. 2011, 2014; Mueller et al. 2017). Our results suggest that climate-related global news is an important risk factor for both exchange rate movements and capital flows.

Lee et al. (2022) find heterogeneous impulse responses of monthly U.S. dollar (USD) real exchange rates of 76 countries to global temperature shocks. We differ from their work in several dimensions: (i) we have a broader cross-section of country pairs; (ii) our climate-related indices move with a broad set of climate-related news, not just realized temperature changes; and (iii) we link both currencies and international current accounts. Javadi et al. (2023) find no link between G10 currencies and the vulnerability of these countries to physical climate risk. Our broader indicator captures both physical and transition risk and suggests the presence of a relevant link at both the daily and the weekly frequency.

Our work is related to the evolving academic field of climate finance (see, among others, Giglio et al. 2021a, b, 2023; Starks 2023; Hsu et al. 2023; Bansal et al. 2019; Pástor et al. 2021, 2022; Colacito et al. 2019; Acharya et al. 2022; Bolton and Kacperczyk 2023, 2021; Bolton et al. 2023; and Kashyap et al. 2024). Recent contributions in this area include Kruttli et al. (2025), who show that firm-level returns are sensitive to extreme weather uncertainty, and Ivanov et al. (2024), who study the effects of cap-and-trade regulation on credit supply. Zhang (2024) documents international variation in carbon return premia, while Shi and Zhang (2025) explore how oil price fluctuations affect the greenium. On the financing side, Albuquerque et al. (2025) highlight the paradoxical effect of green lending on carbon emissions. Finally, Jung et al. (2023) develop measures of physical climate risk exposure using insurer data, illustrating the importance of sectoral sensitivity to climate shocks. The climate macro-finance literature has primarily focused on the link between climate risks, local assets and local macroeconomic dynamics. We differ from these studies for our attention to international quantities and currencies.

2 Climate news shocks in general equilibrium.

We develop a two-period general equilibrium model to derive testable null hypotheses using our novel dataset. The model is designed to capture several key features observed in the data: (i) climate news shocks are priced, (ii) green and brown investments differ in their exposure to climate news shocks, and (iii) countries exhibit heterogeneous sensitivity to common (i.e., global) climate news shocks.

Environment and information timing. The main equilibrium conditions of our model are derived in Appendix C. In what follows, we describe our economic environment and then derive the key predictions regarding stock returns, trade, and currencies. The model features two countries, home and foreign. Foreign variables are denoted by "*". Due to the symmetry of our environment, many of our equations are presented for the home country, with the implicit understanding that they apply to the foreign country as well. Time is discrete and we assume that there are only two periods denoted by the following three dates $t = \{0, 1, 2\}$.

All shocks materialize at the end of the first period, i.e., at $t = 1$. Hence, at time $t = 0$ choices are made under uncertainty. At time $t = 2$, no additional shock materializes, or, equivalently, in the second period there is full resolution of uncertainty. Most importantly, all news received at time $t = 1$ affect the production frontier only at $t = 2$. Hence, from a time-1 perspective, these shocks represent pure news shocks.

Preferences. In each country, the representative household has the following recursive preferences:

$$u_t = (1-\beta)\log\left(\widetilde{C}_t \cdot \mathcal{G}_t\right) + \frac{\beta}{1-\gamma}\log E_t\left[\exp\left\{(1-\gamma)u_{t+1}\right\}\right], \quad t = \{0, 1, 2\},$$

where $\mathcal{G}_t$ captures climate-related sentiment shocks, and $\widetilde{C}_t$ includes both a standard consumption bundle C_t and an endogenous disruption term D_t:

$$\widetilde{C}_t = C_t \cdot D_t^{-1}.$$

The sentiment process evolves as:

$$\mathcal{G}_t = e^{-b \cdot g_t},$$

where g_t is a zero-mean normally distributed global climate news shock. Since periods of heightened climate news coverage (positive g_t) typically reflect unfavorable information about climate risks, a positive realization of g_t reduces the agent's utility. The parameter b (and its foreign counterpart b^*) governs the exposure of each country to global climate sentiment shocks. While this formulation accommodates any sentiment shock, we interpret S_t as a climate-related news shock for two reasons: (i) agents in the economy can hedge this risk by investing in a green technology that mitigates future climate damage, and (ii) the economy is observationally equivalent to one in which S_t represents a news shock about climate disruptions occurring at date $t+1$. Moreover, our model adopts a broad definition of climate sentiment, without distinguishing between shocks associated with physical risk and those linked to transition risk. In our empirical analysis, we leverage text analysis tools to separately identify these two channels.

When $\gamma = 1$, preferences reduce to expected-log utility. For $\gamma > 1$, households exhibit a preference for early resolution of uncertainty, which implies that their marginal utility adjusts immediately in response to new climate news.

In our setting, $\widetilde{C}_0$ and g_0 are predetermined parameters that do not influence the allocation decisions at time $t = \{1, 2\}$. The same logic applies to D_1 and D_1^*, as they are independent of the economic choices made for time $t = 2$. Based on these considerations, we normalize these variables to unity. In addition, we normalize the foreign country's exposure to the global climate sentiment shock to one ($b^* = 1$), so that a value of $b > 1$ indicates that the home country is more sensitive than the foreign country to the same climate news shock. By incorporating this process into the utility function, we capture agents' concerns about climate disruptions, while remaining agnostic as to whether those concerns stem from physical risks or transition risks.

Consumption bundles. We assume that each agent consumes a bundle composed of two consumption goods:

$$C_t = X_t^{\lambda} Y_t^{1-\lambda}, \quad \text{and} \quad C_t^* = X_t^{*(1-\lambda)} Y_t^{*\lambda},$$

where X_t is the home-produced good, and Y_t is the foreign-produced good. The parameter $\lambda > 1/2$ introduces home bias in consumption and ensures that the equilibrium exchange rate is not mechanically pinned to unity. The allocations at times 1 and 2 are determined endogenously through the recursive risk-sharing scheme described below.

Since the model features a finite horizon, we begin the analysis by solving the terminal period and proceed recursively backward.

Time-2 Output and climate disruptions. At time $t = 2$, output in the home and foreign country is given by:

$$GDP_2 = e^{\theta} B, \quad \text{and} \quad GDP_2^* = e^{-\theta} B^*,$$

where $\theta \sim i.i.d. \mathcal{N}(0, \sigma_\theta^2)$ captures a country-specific productivity shock. A positive realization of θ implies that the home country is relatively more productive. The terms B and B^* represent the effective capital stock in the home and foreign country, respectively. These are Cobb-Douglas aggregates of domestic and foreign investment made at time 1:

$$B = I_{x,1}^{\lambda_I} {I_{x,1}^*}^{1-\lambda_I}, \quad \text{and} \quad B^* = I_{y,1}^{1-\lambda_I} {I_{y,1}^*}^{\lambda_I}.$$

We refer to these investments as "brown capital", since they contribute to the severity of future climate disruptions. In contrast, investments in green technology, which help mitigate climate damage, are introduced later in the model.[1] Since the model ends at time 2, there is no further capital accumulation. Thus, all output at $t = 2$ is allocated to consumption goods:

$$GDP_2 = X_2 + X_2^*, \quad \text{and} \quad GDP_2^* = Y_2 + Y_2^*.$$

[1] We let $\lambda_I \neq \lambda$ to allow for the possibility that consumption home bias differs from investments home bias. When $\lambda_I = \lambda$, the structure of the investment bundle mirrors that of the consumption bundle, as in Backus et al. (1994).

The adverse effect that economic activity has on climate conditions is measured by D_t. In our model, only D_2 and D_2^* are endogenous and depend on economic decisions made at time $t = 1$. Specifically, disruptions are modeled as increasing in *brown investments* (captured by GDP) and decreasing in *green investment*, i.e., investment in technologies that mitigate the climate impact of production. Let $I_{g,1}$ and $I_{g,1}^*$ denote green investments in the home and foreign countries, respectively. We assume that home and foreign "green capital" obtain from the following aggregators:

$$G = I_{g,1}^{\lambda_g} I_{g,1}^{*1-\lambda_g}, \quad \text{and} \quad G^* = I_{g,1}^{*\lambda_g} I_{g,1}^{1-\lambda_g}.$$

The disruption terms take the following form:

$$D_2 = \left(\frac{GDP_2^{\lambda_g} \cdot GDP_2^{*1-\lambda_g}}{G} \right)^a, \quad D_2^* = \left(\frac{GDP_2^{*\lambda_g} \cdot GDP_2^{1-\lambda_g}}{G^*} \right)^a,$$

where the parameter λ_g governs the relative importance of domestic versus foreign sources of disruption. When $\lambda_g = 0.5$, agents are equally concerned about domestic and foreign drivers of climate deterioration. When $\lambda_g > 0.5$, local disruptions lead to stronger deterioration of local utility. Disruptions should be interpreted broadly, as including both potential physical damages and distortions due to transition risk. The parameter a satisfies the restriction $0 < a < 1$.

Time-1. At time $t = 1$, output is predetermined and normalized to 1 in each country for simplicity. The corresponding resource constraints reflect the possibility of international trade in both consumption and investment goods:

$$1 = X_1 + X_1^* + I_{x,1} + I_{y,1} + I_{g,1}, \quad 1 = Y_1 + Y_1^* + I_{y,1}^* + I_{x,1}^* + I_{g,1}^*.$$

From the home (foreign) country's perspective, $I_{x,1}$ ($I_{y,1}^*$) represents local investment, while $I_{y,1}$ ($I_{x,1}^*$) reflects investment abroad. Although capital stocks are country-specific, agents can trade both consumption and brown investment goods across borders without frictions in every state of the world, consistent with the setting in Colacito et al. (2018). Green investments are inherently local and cannot be traded internationally. For instance, an afforestation project undertaken in the home country cannot simply be relocated to a foreign country. Nonetheless, these investments have global impli-

cations: although undertaken locally, they enter symmetrically into both countries' disruption functions, D_2 and D_2^*, thus reflecting shared climate benefits.

The two countries are assumed to begin with a balanced net foreign asset position at time $t = 0$. Right before the realization of shocks at time $t = 1$, households can trade a complete set of Arrow-Debreu securities, which allows them to hedge their specific exposure to both productivity and climate news shocks. Since all uncertainty is resolved at time $t = 1$, no additional trading of these securities occurs after this period.

In addition, we assume that potential externalities are fully internalized through international carbon taxes and subsidies. This allows the allocation to be derived from a planner's problem using the methodology developed by Colacito et al. (2018). In a recursive risk-sharing scheme, agents care not only about the expected value of their future utility, but also about how their hedging decisions affect its conditional variance. To see this point, notice that when continuation utilities are approximately log-normal, the following holds:

$$u_t \approx (1-\beta)\log\left(\widetilde{C}_t \cdot \mathcal{G}_t\right) + \beta E_t\left[u_{t+1}\right] + \beta\frac{(1-\gamma)}{2}V_t\left[u_{t+1}\right].$$

This formulation shows that agents care not only about the expected value of future utility but also about its conditional volatility. From the perspective of time 0, countries with greater exposure to global climate news—i.e., higher b—face more uncertainty about their continuation utility. As a result, these agents have a stronger incentive to hedge against the realization of adverse climate news shocks at time 1. To hedge this risk, the more exposed country buys insurance that pays off in states where the climate news shock g is positive. When such a shock materializes, this country can import resources from abroad (resulting in negative net exports), and its currency appreciates.[2] Equivalently, when climate news shocks affect future welfare, they are priced and affect international trade in equilibrium.

[2]In practice, we must solve a fixed-point problem: the optimal asset trade depends on the distribution of continuation utilities, but that distribution is itself determined endogenously by the chosen trading strategy. Appendix C provides the detailed derivation of this recursive risk-sharing equilibrium.

Returns. We are interested in comparing the market value of assets before and after the realization of the shocks θ and g at time $t = 1$. Since in this economy all cash-flows are paid out at time $t = 2$, we can define the returns after the realization of the shocks as follows:

$$r_{i,1|0} := \log R_{i,1|0} = \log \frac{Q_{i,1}}{Q_{i,0}}, \quad i \in \{b, g\}, \tag{1}$$

where $Q_{i,t}$ denotes the time-t ex-dividend value of the marginal cash-flows paid out by investment in the final period of the model. We denote brown and green investment by $i \in \{b, g\}$, respectively. The valuation $Q_{i,0}$ is predetermined in this economy, i.e. it can be taken as given. As a result, the return dynamics depend solely on $Q_{i,1}$, which reflects the market value of cash flows from the perspective of time 1. In general equilibrium, the $t = 1$ present value of future cash-flows must equal the marginal cost of additional installed capital. Hence, we can use marginal Tobin's Q for brown and green investments to characterize the response of:

$$r^{bmg}_{1|0} := r_{b,1|0} - r_{g,1|0} = constant + (1 - \lambda_I) \log \frac{I_{x,1}}{I^*_{x,1}} - (1 - \lambda_g) \log \frac{I_{g,1}}{I^*_{g,1}}.$$

2.1 Testable hypotheses.

In what follows, we present three propositions that guide our empirical analysis. All proofs are provided in Appendix C. The first two propositions concern the behavior of currencies and asset returns, and can be tested using high-frequency data. The third proposition pertains to the dynamics of international current accounts, which we evaluate using quarterly data. In this section, we focus exclusively on the role of climate news shocks. However, our full model also incorporates an endogenous link between productivity news and climate disruption, consistent with standard integrated assessment frameworks. Detailed analytical derivations are provided in the Appendix.

We state our propositions in the most general way and we use results obtained under additional parametric restrictions in order to provide additional intuitions. Without loss of generality, when presenting analytical formulas, we use the following assumption.

Assumption 1. *The following parametric restrictions hold:* $a \in (0,1)$*,* $\gamma > 1$*,* $\lambda = \lambda_I = \lambda_g \in (0.5,1)$ ***and*** $\beta \in (0,1)$*.*

In this class of risk-sharing models, the allocation at time $t = 1$ moves with an endogenous state variable called ratio of the pseudo-Pareto weights. At time $t = 1$, this variable is denoted as $\widetilde{S}_1$. At time $t = 0$, this variable is normalized to 1, implying that the two countries have the same relative size before the realization of the shocks. In practice, $\widetilde{S}_1$ measures the transfer that the home country receives from the foreign country in each state. More specifically, the home country ex-ante hedges itself against bad shocks and receives ex-post a higher $\widetilde{S}_1$ if bad news is realized. In our simplified setting, the log-ratio of the Pareto weights at time $t = 1$ is approximately equal to:

$$\begin{aligned} \tilde{s}_1 = \bar{s} \quad &+ \quad \tilde{\beta} \cdot (\gamma - 1) \cdot \left(\frac{(b-1)a}{1 + 2(\gamma - 1)\lambda_u^s} \right) \cdot g \\ &- \quad \tilde{\beta} \cdot (\gamma - 1) \cdot \left(\frac{(1-a)(2\lambda - 1)}{1 + 2(\gamma - 1)\lambda_u^s} \right) \cdot 2\theta, \end{aligned} \tag{2}$$

where $\tilde{\beta} = \beta(1-\beta)$, and both $\lambda_{Ix}^S > 0$ and $\lambda_u^s > 0$ are composite positive parameters. If preferences are not time-additive ($\gamma > 1$), the log-ratio of the Pareto weights $\tilde{s}_1$ increases in response to an adverse sentiment shock ($g > 0$) and it decreases in response to a positive productivity shock ($\theta > 0$).

Proposition 1. *Let* $\gamma > 1$*, when* $b > 1$ *(*$b < 1$*), a global climate news shock* $g > 0$ *causes an appreciation of home (foreign) real exchange rate.*

In our model, the log-growth rate of the exchange rate at date $t = 1$ evolves as follows

$$\Delta e_1 \quad = \quad \overline{\Delta e} + \lambda_e^s \cdot \tilde{s}_1. \tag{3}$$

In our simplified calibration,

$$\lambda_e^s \quad = \quad (2\lambda - 1)^2 \cdot \left[1 - 2\frac{\beta}{1+\beta}(1-\lambda)(1-a) \right] > 0, \tag{4}$$

implying that the exchange rate appreciates in response to an adverse sentiment shock ($g > 0$) and it depreciates in response to a positive productivity shock ($\theta > 0$).

Intuitively, Proposition 1 implies that adverse global climate news shocks lead to an appreciation of the currencies of countries that are relatively more exposed to such news. This occurs because, when the shock materializes, the investors in these countries have a relatively higher marginal utility. Under complete markets, this translates into an increase in $\widetilde{S}_1$ and a stronger real exchange rate.

Proposition 2. *Let $\gamma > 1$. If $b > 1$, the brown-minus-green investment return in the home country depreciates when there is a positive global climate news shock g, i.e., $\frac{\partial r_{1|0}^{bmg}}{\partial g} < 0$. In addition, the effect is stronger with a higher b, i.e., $\frac{\partial^2 r_{1|0}^{bmg}}{\partial g \partial b} < 0$.*

The log-return of brown stocks in excess of green stocks at date $t = 1$ is equal to:

$$r_{1|0}^{bmg} = \bar{r} + \lambda_{r^{bmg}}^{s} \cdot \tilde{s}_1, \tag{5}$$

where, in our simplified setting,

$$\lambda_{r^{bmg}}^{s} = (1 - \lambda)(1 - 2\lambda) < 0.$$

It follows that the excess return declines in response to a positive sentiment shock ($g > 0$) and it increases in response to a positive productivity shock ($\theta > 0$). In addition, since the elasticity of the ratio of the pseudo-Pareto weights is increasing in $b - 1$ (see equation (2)), the exposure of the $r_{1|0}^{bmg}$ is relatively more negative when the brown firm is located in highly exposed countries (higher b). This finding motivates the use of an *interaction* term between firm-level emissions (a common measure of firm's brown-ness) and country exposure in our regressions (equations (9) and (10)).

The next and last proposition focuses on international hedging via international trade.

Proposition 3. *Let $\gamma > 1$, when $b > 1$, a global climate news shock $g > 0$ decreases total net exports in the home country, implying that there is a reallocation of resources toward the country that ex-ante hedges the most.*

A positive climate news shock, $g > 0$, reveals adverse information about future global climate conditions and it leads to a decline in net exports for the country that is more exposed to such shocks, i.e., the country with a higher b coefficient. In this state of the world, without trade the more exposed country would experience a larger

increase in marginal utility and would be therefore worse off. To restore equality in marginal utilities under optimal risk-sharing, the most exposed country hedges ex-ante and receives a transfer of resources from the less exposed one ex-post. In the decentralized economy, this transfer corresponds to higher imports and lower exports, leading to a decline in net exports of the home country. This pattern is a direct implication of the recursive risk-sharing equilibrium under complete markets as the net exports move together with $\widetilde{S}_1$. In the data, we test this result by looking at country pairs sorted according to our estimated exposure to the global climate attention index.

3 Data

Data collection. In line with the methodology developed in Engle et al. (2020), we construct a climate attention index to assess the extent of discourse concerning climate change within the news media. Our approach differs from that of Engle et al. (2020) in that we have chosen to focus on news media outlets, particularly newspapers, that have a strong presence on the social media platform Twitter.[3] Utilizing textual analysis, we generate country-level indices at both low and high frequencies. As of the date of this draft, our dataset encompasses a total of 25 countries, providing a comprehensive representation across a wide spectrum of local languages, income levels, and geographical regions. We have conveniently summarized our dataset in Table 1.

In what follows, we describe the construction of our climate attention index. In a second step, we show that in the data we can disentangle attention to topics related to physical risk and transition risk. Importantly, we document that spikes in climate attention are associated with news carrying negative sentiment. Based on this observation, we use the terms “high climate attention” and “negative climate sentiment” interchangeably throughout the remainder of the analysis.

[3]Our data collection ended in December 2022. The platform is currently identified as "X". The list of newspapers included in our data set can be found in the appendix. The selection of newspapers was determined through a two-step process: first, we verified whether the newspapers had been included in prior studies (Baker et al. 2016) and were categorized as primary information outlets. Second, we expanded upon this criterion by evaluating whether each newspaper's Twitter handle had a substantial number of followers and maintained consistent posting activity.

TABLE 1. DATASET SUMMARY

Country	Tot. no. News Outlets	Tot. no. Tweets	Tot. no. Words	Tot. no. Terms	Language
AR	4	1,892,464	16,592,918	50,513	Spanish
AU	4	539,792	5,805,411	46,253	English
BR	3	1,091,173	9,157,179	46,841	Portuguese
CA	5	1,071,360	9,662,873	48,695	English
CH	4	312,897	2,477,651	40,932	German and French
CL	3	1,088,455	9,422,589	48,409	Spanish
CN	3	488,076	6,786,626	53,342	English
CN (HK)	2	305,490	2,982,160	28,143	English
CO	3	1,291,773	10,348,974	55,984	Spanish
DE	4	708,692	6,779,556	31,190	German
ES	4	1,484,502	13,662,696	61,176	Spanish
FR	4	1,004,595	8,950,751	54,021	French
IN	4	1,909,474	22,370,252	71,505	English
IT	3	1,268,190	10,209,216	42,084	Italian
JP	4	353,247	3,819,349	36,544	English
KR	4	302,946	2,814,363	28,923	English
MX	4	2,041,505	19,553,684	70,880	Spanish
NO	3	152,521	921,258	13,022	Norwegian
NZ	3	147,218	1,156,784	20,538	English
PT	3	802,011	6,102,651	40,929	Portuguese
SA	3	914,623	8,754,709	44,571	Arabic
SE	4	190,493	1,607,852	19,201	Swedish
UK	4	791,929	6,978,125	46,460	English
US	11	2,735,338	29,141,511	72,662	English
ZA	3	453,135	3,945,579	33,473	English
Total	**96**	**23,341,899**	**220,004,717**	**1,106,291**	

Notes: This table shows summary statistics for all news that we collect for a large cross section of countries. Our real-time data range from 1/10/2014 to 31/12/2022. For each country, we report the total number of Twitter accounts that we monitor (major newspapers and other media outlets), the total number of tweets collected, total number of words, total number of unique terms (accounting for unigrams and bigrams), and original language. We translated the corpus in Engle et al. (2020) to 8 different languages, in order to construct our index.

Climate attention index construction. We use the "universe" of Tweets from October 2014 until December 2022 from the Twitter accounts of official newspapers (the full list of newspapers is reported in table A.1 in the appendix). We construct our index by comparing the news content in these tweets to a corpus of "[...] authoritative texts on the subject of climate change" as in Engle et al. (2020). Similar to Engle et al. (2020), we aggregate the authoritative text documents into a Climate Change

Vocabulary (CCV), which amounts to the list of both unique terms and their associated frequency with which each one of them appears in the aggregated corpus. In the construction of our dataset, we use the text (if any) of the Twitter posts and not the respective articles. Before doing so, we preprocess both the corpus of authoritative texts and the newspaper's tweets. The preprocess removes (1) any links, (2) any tags to Twitter accounts, (3) any special characters and/or numbers, and (4) stop words (e.g, "and" "or"). Furthermore, it stems each word (using the Snowball algorithm), and it keeps only words with more than two characters. The stemming procedure retains only the root of each terms; for example, terms like "work" and "working" are included as unique terms. See Figure A.1 in the appendix for a word cloud representation of the preprocessed corpus in English.

Second, we construct the analogous count from our preprocessed Twitter texts for every country. Our approach enables us to construct our measures both at high and low frequency. When studying the impact of climate attention shocks on currencies, we use a daily aggregation method. In what follows, we focus on monthly aggregation of tweets for illustrative purposes. We refer to the Twitter texts aggregated in a specific month for a specific country as "document". At the monthly frequency, we have a total of 99 documents for each country. Next, we convert the term counts from each one of our documents into term frequency–inverse document frequency scores (in short, "tf-idf" scores). Finally, for each document, we compute the cosine similarity between its tf-idf scores and those of the entire corpus. We carry out the described procedure for every country within our sample.

In cases where a country uses a language other than English, we employ the Google Translate API to translate the original English corpus into the appropriate foreign language. These languages include German, Spanish, French, Norwegian, Swedish, Arabic, Portuguese, and Italian. This approach enables us to create Climate Change Vocabulary (CCV) sets for each of the available languages, facilitating the analysis of newspapers published in local languages. This approach mitigates the potential news bias that might arise from solely relying on English-language newspapers in non-English-speaking countries.[4] For countries with multiple local languages, such as Switzerland, we generate an index for each language and calculate the average

[4]For China, Japan and Korea, we retained the English-speaking newspapers posts due to the challenges in preprocessing languages with special characters. Our results are robust to the removal of these countries.

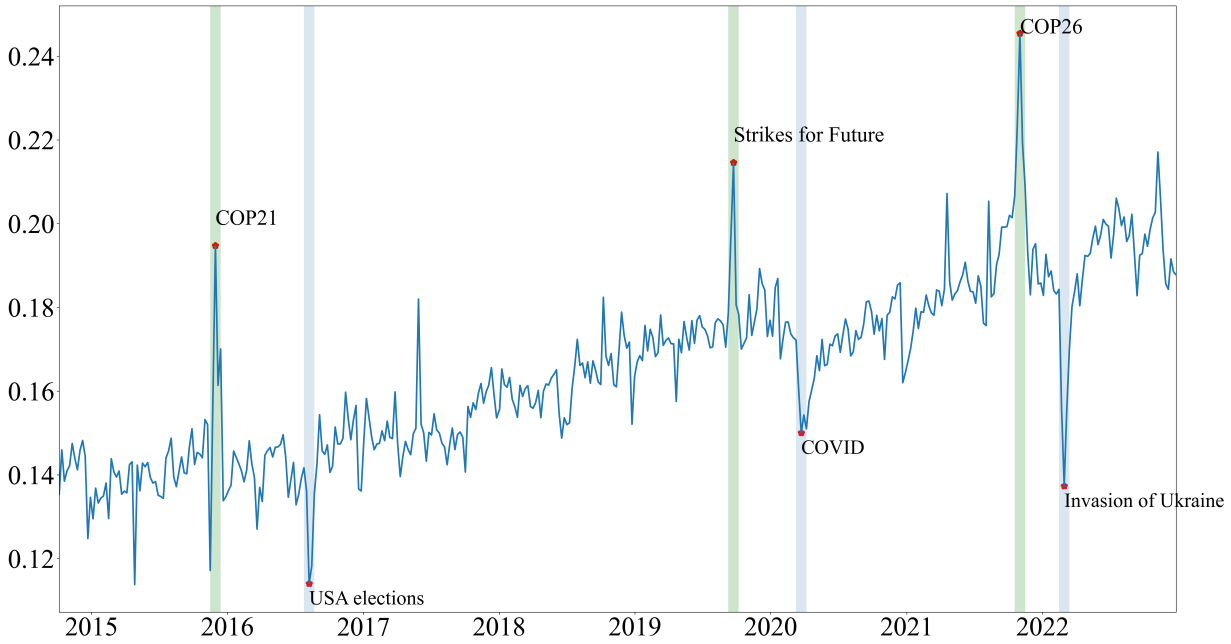


FIG. 1. WORLD CLIMATE ATTENTION INDEX (CAI)

Notes: This figure shows our Global Climate Attention Index. It is based on the methods described in section 3 applied to the countries listed in table 1 and a total of 8 languages.

across these indices.

Figure 1 presents our weekly Climate Attention Index (CAI), which has been aggregated across countries. The index is constructed by taking the equally weighted average across all the countries in our sample. The calculation of the index at the country-level is necessary because we cannot mix documents written in different languages. Consolidating documents at the country-language-frequency level would yield highly comparable results.

Our index effectively reflects specific global events. For instance, the United Nations Climate Change Conference (COP26), held in early November 2021 with the aim of promoting commitments to combat climate change, garnered significant attention worldwide, as evident in our index. Conversely, the COVID-19 pandemic and the invasion of Ukraine had the opposite effect on our index, with a notable decline attributed to a reduced proportion of climate-related discussions during these periods. Typically, significant events like elections, conflicts, and health crises tend to lead to a decrease in our index.

Heterogeneous sensitivity to global climate news. Figure 2 illustrates the same index across all of the countries included in our dataset. One of the novelties of our dataset is that it spans a large cross-section, which enables us to measure heterogeneity across countries. In the spirit of the international macro-finance literature, in what follows we focus primarily on heterogeneous exposures to global shocks (see Lustig et al. (2011)).

Specifically, let $CAI_{i,t}$ denote the index for country i at time t. The world climate attention index is defined as follows:

$$\overline{CAI}_t = \sum_i \omega_{i,t} CAI_{i,t}, \tag{6}$$

where $\omega_{i,t}$ is a country-specific weight. We provide results based on three alternative weighting schemes: (i) by equally weighting all countries, (ii) by weighting each country proportionally to its share of global GDP, and (iii) by weighting each country proportionally to its share of Twitter volume. Volume weights are based only on tweets with a similarity score with the corpus of authoritative text above median. Equivalently, we only include the volume of tweets that are the most relevant for the focus of our analysis. We then estimate the following regression:

$$\Delta CAI_{i,t} = \beta_i \cdot \Delta \overline{CAI}_t + u_{i,t}, \tag{7}$$

where Δ refers to a demeaned growth rate over time for each country. We regard β_i as a measure of exposure to a common, i.e., global, component, and $u_{i,t}$ as a pure local component. Equivalently, we interpret β_i as the empirical counterpart of b in the model, that is, the parameter that determines how much a country is sensitive to global climate news shocks.

Table 2 presents the estimated β parameters for each country in our sample under various weighting schemes for the global CAI index. These β values exhibit a strong positive correlation across different weighting schemes, with correlation coefficients exceeding 0.9. Using the equally weighted global CAI index as the reference, we observe that South Korea, Saudi Arabia, China (including both Hong Kong and Mainland), and Japan consistently possess the highest β values. Conversely, Switzerland, South Africa, Chile, Norway, and Germany consistently exhibit the lowest β

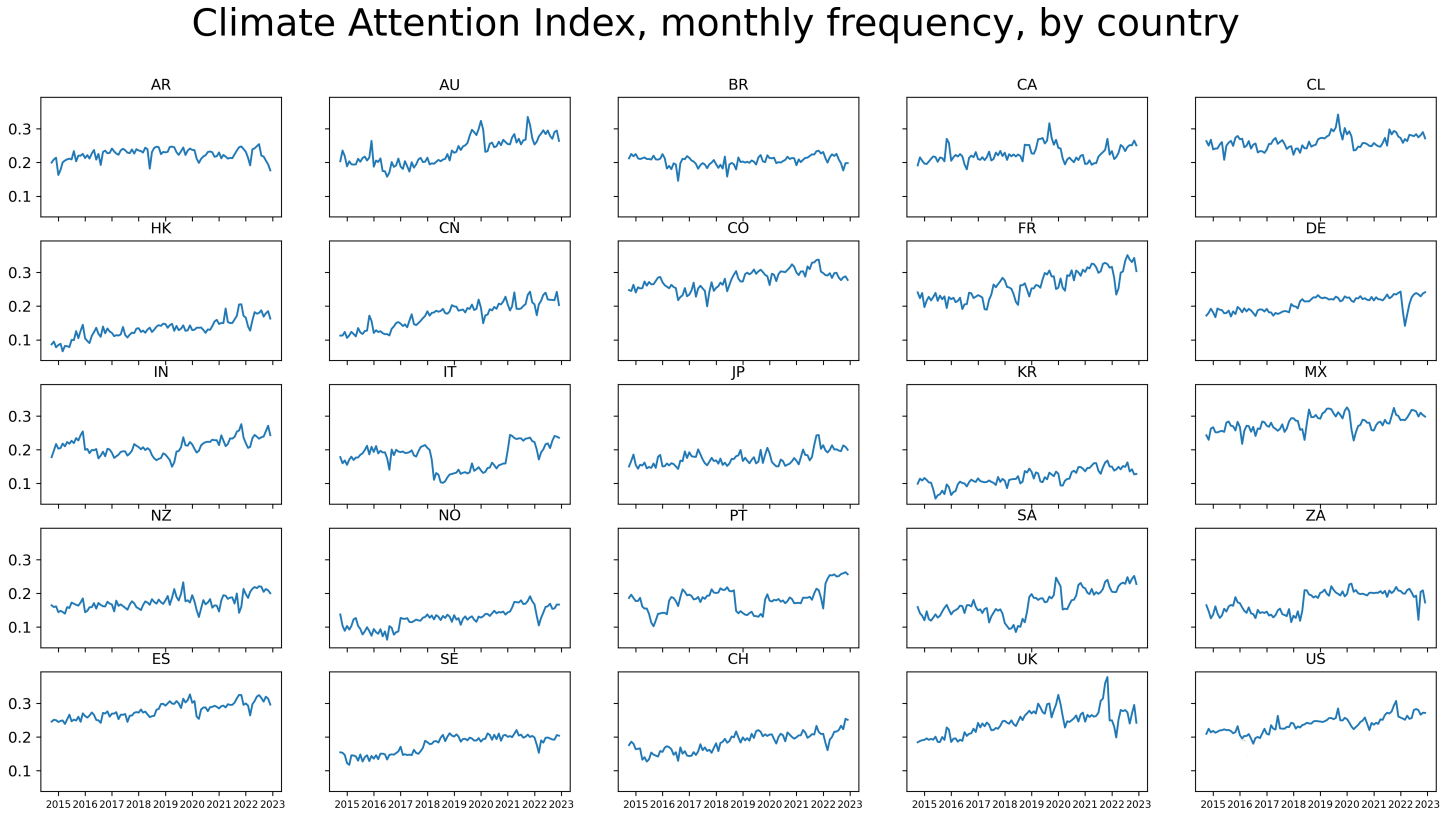


FIG. 2. WORLD CLIMATE ATTENTION INDEX (CAI) BY COUNTRY

Notes: This figure shows our Global Climate Attention Index. It is based on the methods described in section 3 applied to the countries listed in table 1 and 8 languages. For countries with multiple languages (e.g., Switzerland), the country-level index is the average of each language index.

TABLE 2. ESTIMATED β FOR EACH COUNTRY

	Equally weighted		GDP weighted		Volume weighted	
Country code	β	s.e.	β	s.e.	β	s.e.
AR	0.929	0.209	0.574	0.148	1.047	0.246
AU	1.419	0.197	0.932	0.190	1.375	0.219
BR	0.616	0.293	0.470	0.218	0.717	0.294
CA	1.710	0.224	1.312	0.138	1.789	0.232
CL	0.241	0.285	0.113	0.175	0.262	0.291
CN (HK)	2.105	0.325	1.196	0.326	1.619	0.518
CN	2.014	0.344	1.787	0.142	1.887	0.450
CO	0.679	0.180	0.561	0.115	0.702	0.207
FR	0.662	0.247	0.320	0.243	0.712	0.274
DE	0.363	0.122	0.236	0.074	0.316	0.160
IN	1.410	0.367	1.144	0.184	1.547	0.330
IT	0.985	0.593	0.624	0.473	1.441	0.705
JP	1.895	0.271	1.472	0.236	1.750	0.233
KR	2.413	0.394	1.624	0.280	1.889	0.324
MX	0.613	0.243	0.376	0.141	0.847	0.244
NZ	0.811	0.293	0.428	0.223	0.767	0.318
NO	0.344	0.320	0.245	0.267	0.166	0.313
PT	0.469	0.663	0.083	0.432	0.130	0.614
SA	2.266	0.574	1.108	0.251	2.254	0.609
ZA	0.197	0.466	-0.029	0.466	0.063	0.612
ES	0.534	0.128	0.366	0.084	0.578	0.114
SE	0.592	0.251	0.255	0.116	0.394	0.208
CH	-0.028	0.414	-0.014	0.263	-0.168	0.335
UK	0.993	0.269	0.798	0.214	0.998	0.339
US	0.768	0.143	0.743	0.083	0.905	0.134

Notes: This table reports the estimated β_i reported in equation (7), that is, the country-specific exposure to the global climate attention shock. The global climate attention shock is constructed as the equally weighted, GDP-weighted, and Twitter volume-weighted cross-sectional average at each point in time. Volume- and GDP-based weights are lagged by one period. The sample ranges from 2015:Q1 to 2022:Q4. Standard errors are HAC-adjusted.

values. The relevance of this heterogeneity is twofold. First, the model suggest that climate news shocks impact currencies and international trade when countries have heterogenous sensitivities ($b \neq b^*$). Our cross section features 138 country-pairs with exposures to the global CAI that are different from each other at the 10% confidence level.

Second, this cross section is *distinct* from common measures of vulnerability and exposure to physical risk. Specifically, we assess the correlation between our estimated β values and alternative measures of climate exposure. We first use the vulnerability score provided by the Notre Dame Global Adaptation Initiative. This index aims to encapsulate "a country's exposure, sensitivity, and capacity to adapt to the negative effects of climate change." We calculate the average of these scores over the longest available period (1995-2021). The upper panel of Figure 3 illustrates the relationship between our β estimates and the vulnerability score. We observe a positive and statistically significant correlation between our β estimates and this index, implying that countries with greater susceptibility to climate change usually exhibit higher β values, i.e, more attention exposure to global climate news. Importantly, a large share of the variance in our cross section is not explained by vulnerability.

Second, we relate our estimated β values to absolute latitude. Generally, countries situated in regions with higher absolute latitudes are usually considered less exposed to rising temperatures resulting from climate change. To assess this, we compile a dataset of city-level absolute latitudes for each country and compute the population-weighted average of these latitudes. Our analysis reveals a weak negative correlation between our β estimates and absolute latitude.

In the context of our model, the vulnerability of the home country is captured by its disruption functions, D, while its sensitivity to global news shocks is governed by the country-specific parameter b. In the next section, we show that our estimated exposure coefficients provide information beyond what is captured by vulnerability alone. Equivalently, the coefficients β_i serve as empirical proxies for the model's sensitivity parameter b, and they highlight a novel finding: attention to global climate news can be high even in countries with low vulnerability, with significant implications for exchange rates, asset prices, and trade.

Top days. In the next section, we use high-frequency data to identify the impact of climate news shocks on exchange rates and stock returns. To identify innovations in our global index, we initially calculate the daily growth rate in the raw CAI index for each country and subsequently remove its mean. These demeaned indices at the country level are then winsorized at the 99.9% and aggregated to generate a global

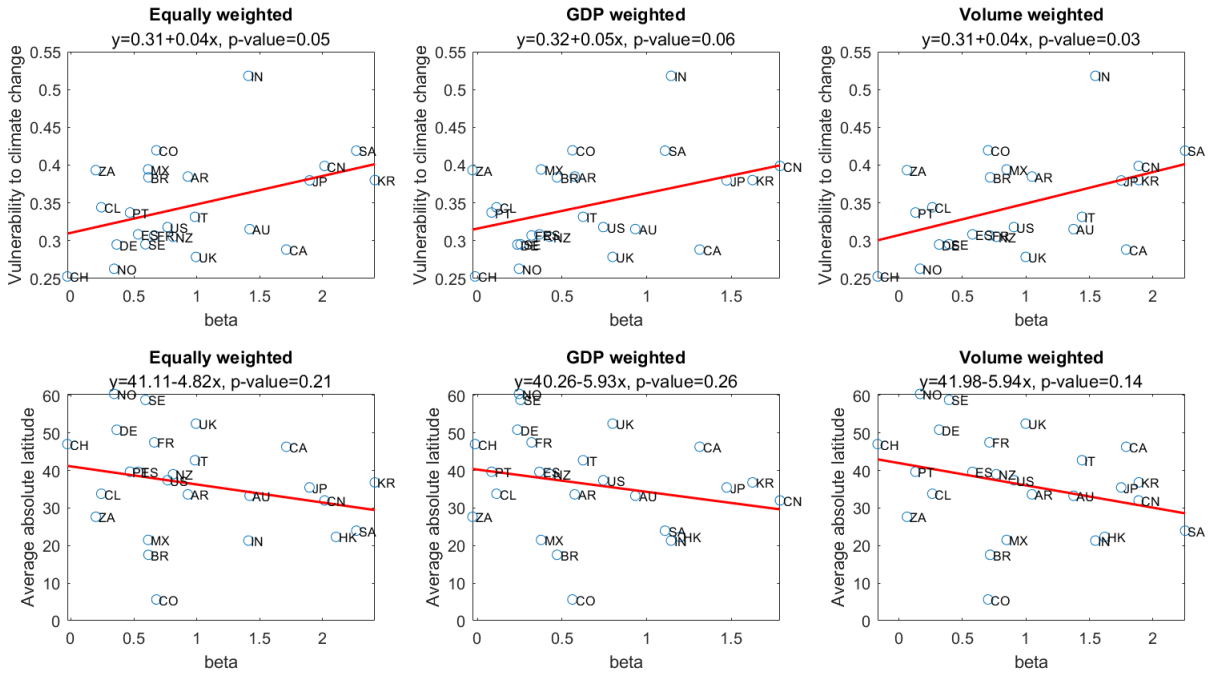


FIG. 3. β AGAINST VULNERABILITY TO CLIMATE CHANGE.

Notes: This figure shows the scatter plot of the estimated βs in equation (7), and measures of vulnerability to climate change across countries. The βs are estimated using the global climate attention shock constructed as either the equally-, GDP-, or Twitter volume-weighted cross-sectional average at each point in time. The upper panels consider each country's average vulnerability score from the Notre Dame Global Adaptation Initiative. The lower panels refer to the average absolute latitude of each country, that is, a population-weighted average absolute latitude of all cities in each country. City-level latitudes are collected from the World Cities Database.

metric.[5] The outcomes of this analysis are visualized in Figure 4.

Based on the distribution of innovations in our global climate index, we select the top 15% of these innovations.[6] Specifically, we examine the reaction of currencies and stocks in the days following a substantial increase in climate attention. This approach serves two purposes: (i) to minimize noise from news unrelated to climate, and (ii) to more effectively identify days driven by "pure" climate news shocks. Such a methodology is commonly used in the literature investigating the effects of news

[5]When we compute our index at the daily frequency, it is possible that in some days and for some countries we could have extreme growth rates because our index gets close to zero. We remove both the top- and bottom-0.1% realizations from our sample.

[6]We analyze the distribution of news for each day of the week, which allows us to account for any patterns specific to particular days (e.g., Monday or Friday effects). This approach is standard in studies focusing on daily news.

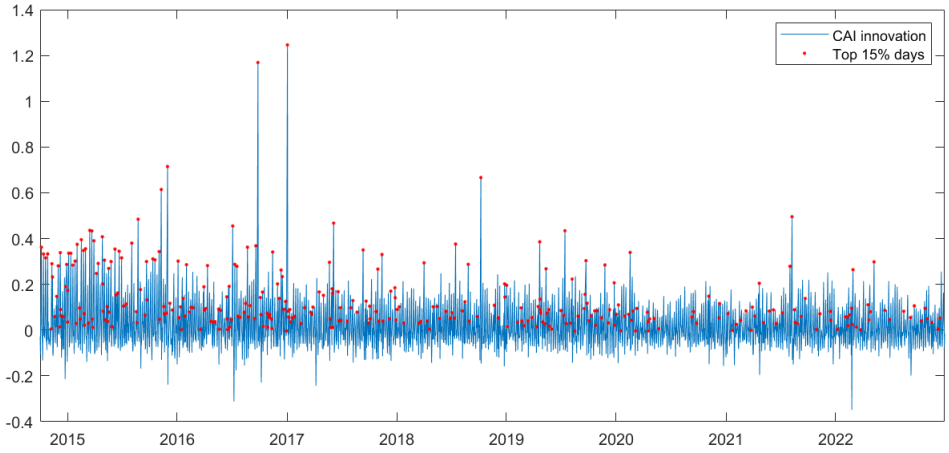


FIG. 4. INNOVATIONS TO WORLD CLIMATE ATTENTION INDEX (CAI)

Notes: This figure shows innovations to our equal-weights Global Climate Attention Index constructed as described in section 3. Our cross section of countries is reported in table 1. Country-level indices are aggregated using equal weights. Red dots are classified as climate-related news days (top-15% realizations). Weekends are excluded.

related to policy announcements (see, for instance, Leombroni et al. (2021)). It is worth noting that some days with a high volume of climate-related news may fall below our top 15% threshold due to the dominance of other topics in the news. As a result, similar to previous studies, this procedure may introduce a downward bias, making it less likely to detect a significant effect of climate news on asset prices and currencies.

Volume for top-days. In principle, one could be concerned that our top-days represent days with no significant global non-climate events. That is, our "climate-focused" days may actually just be "news vacuums" days. In order to address this concern, we regress global weekday tweet-volume on a top-day dummy, as well as country, year, month, and weekday dummies. Untabulated results show that the implied coefficient in front of our top-day dummy is both small (the point estimate refers to 1 tweet) and insignificant (we use a two-way-clustered specification by country and day). Hence, after accounting for seasonality in the news cycle, our top-day dates are not slow news days, but rather days in which the news shift toward climate.

Topics for top days. After identifying top-attention days, we examine the content of the news shared during these periods. Following the text analysis literature (see, for example, Hassan et al. (2019)), we employ a pre-trained sentence embedding model to extract semantic representations of newspaper tweets. These embeddings are then clustered to identify a smaller set of key themes, or main topics. This dimensionality reduction enables the use of topic-level cosine similarity scores to classify tweets as climate-related and further distinguish between those primarily associated with physical risk and transition risk. The process involves several carefully designed steps aimed at minimizing discretion on our part, which we detail below.

First, we generate 100 climate risk-related sentences using ChatGPT: 50 focused on physical risks (e.g., extreme weather) and 50 on transition risks (e.g., regulatory changes). The full list of these sentences is provided in Table A.2 in the Appendix. Next, we analyze the identified top climate-attention days by preprocessing raw newspaper tweets, removing non-informative elements such as links and special characters. We then convert the cleaned tweets into high-dimensional vector representations (sentence embeddings), which serve as inputs for the BERTopic clustering algorithm (see Grootendorst (2022)).[7]

After identifying the key topics discussed in the media on these top-attention days, we compute cosine similarities between each topic embedding and each AI-generated sentence embedding. This approach allows us to assess how closely each topic aligns with climate-related themes. Specifically, a topic is classified as climate-related if its cosine similarity score with any AI-generated climate sentence falls within the top 0.1% of the score distribution (with a threshold of 0.546). Using the 99.9^{th} percentile ensures a stringent definition of climate-related topics.

Finally, we classify each climate-related topic as either "Physical Risk" or "Transition Risk" based on its closest match to the sentences listed in Table A.2. If the most related sentence corresponds to physical (transition) risks, the topic is labeled accordingly. Figure 5 visualizes the most frequent words in these two groups of tweets, with

[7]BERTopic is a topic modeling technique that integrates transformer-based embeddings with clustering to extract coherent topics from large text datasets. We use the package provided at https://maartengr.github.io/BERTopic/index.html. We keep the following default options: (i) UMAP (Uniform Manifold Approximation and Projection) with five components, and (ii) HDBSCAN (Hierarchical Density-Based Spatial Clustering of Applications with Noise) to group tweets into distinct topics. Since our data comprise tweets in different languages, we must use the embedding model "distiluse-base-multilingual-cased-v2" by Reimers and Gurevych (2019).

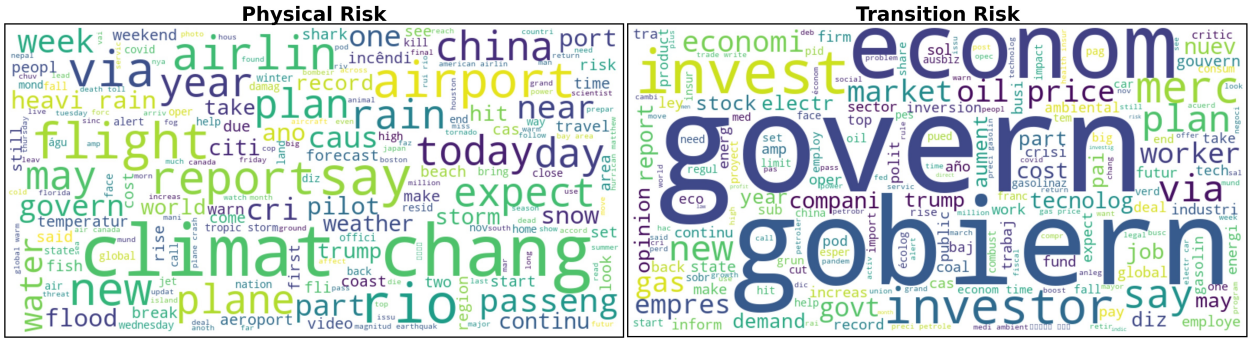


FIG. 5. WORDCLOUD OF CLIMATE-RELATED TWEETS DURING TOP DAYS.

Notes: This figure shows the word cloud of root words extracted from climate-related Tweets in our sample of top days. Tweets are classified as climate-related if the cosine similarity of their associated topic exceeds the 99.9th percentile of the similarity scores calculated against a set of AI-generated reference sentences. Tweets are further classified as physical (transition) risk if their topic aligns most closely with a physical (transition) risk-related sentence (see table A.2). Our sample period starts in October 2014 and ends in December 2022. Transition risk generally refers to risks arising from changes in policies, technologies, and market preferences associated with climate action. Physical risk relates to the direct impact of climate change, such as extreme weather events and rising temperatures.

the resulting word clouds reinforcing our methodology by clearly distinguishing between different sources of climate-related concerns. In the following analysis, we use these two groups of tweets in both our sentiment analysis and high-frequency asset pricing analysis.[8]

Sentiment of tweets. We analyze the sentiment of climate-related tweets during top days by using the Twitter-XLM-RoBERTa model from CardiffNLP.[9] This is a transformer-based multilingual sentiment classifier suitable for text in multiple languages (Barbieri et al. 2022). Each one of our tweets is tokenized and passed

[8]ClimateBERT (see Webersinke et al. (2022)) is a natural candidate for analyzing climate-related text, given its domain-specific training. However, we chose not to use it for our analysis due to two key limitations. First, ClimateBERT is trained exclusively on English-language text, which poses challenges in our context where the dataset spans multiple countries and includes tweets in a variety of languages. Translating all non-English content into English could introduce distortions that bias the analysis, particularly when dealing with linguistic nuances or compressed phrasing typical of headline-style content shared by news outlets on social media. Second, ClimateBERT was originally pretrained on longer, formal texts such as news articles, research abstracts, and corporate disclosures, and was not explicitly optimized for short-form content like tweets or headlines. As a robustness check, we compared the share of physical risk tweets identified by our model to the share of tweets classified as such by both ClimateBERT and our model for U.S.-based content, and found a correlation of approximately 80%.

[9]Available at https://huggingface.co/cardiffnlp/twitter-xlm-roberta-base-sentiment.

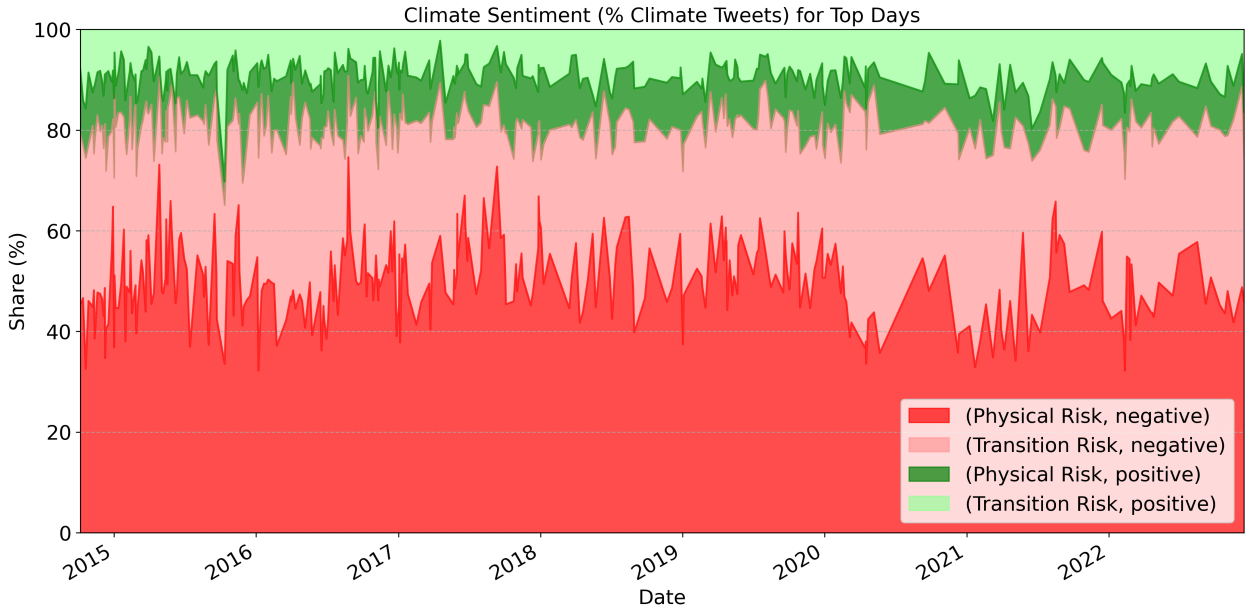


FIG. 6. SENTIMENT OF CLIMATE RELATED TWEETS DURING TOP DAYS.

Notes: This figure presents the share of climate-related tweets categorized by sentiment (positive or negative) and risk type (transition or physical) on days for which there is a positive spike (top-15%) in the global CAI innovations. The sentiment classification is based on a multilingual sentiment classifier Barbieri et al. 2022). The word clouds for transition and physical risk are reported in figure 5.

through the pre-trained model in order to obtain a sentiment label (negative, neutral, or positive) based on the highest logit value.

Figure 6 presents the share of climate-related tweets in each risk category (physical and transition) that are classified as either positive or negative. In our sample, global news shocks related to climate typically have a negative tone. Equivalently, our top-attention days are usually bad-news days.

4 Climate News Shocks and Asset Prices

In this section, we explore the role of climate news shocks for currencies and equity returns.

4.1 Exchange Rates

In what follows, let $\Delta e_{(H,F)} > 0$ refer to an appreciation of the currency of country H versus country F. Proposition 1 states that countries with higher sensitivity to climate news should experience a currency appreciation if adverse news materialize.

In order to test this condition, we obtain bilateral exchange rate data from Bloomberg and sort our country pairs as follows. Let H and F be two countries in a country-pair. For every non-repeated pairwise combination of countries, $i \neq j$, we look at the exposure of the country-specific CAI to the global CAI as estimated in equation (7). If $\beta_i - \beta_j > 0$ ($\beta_i - \beta_j < 0$) we denote country i as H and j as F (j as H and i as F) and focus on the exchange rate $e_{(H,F)}$.

We test this assumption at a high-frequency level, particularly on days when climate-related news is exceptionally significant. Figure 7 illustrates the average cumulative exchange rate variation following these specific days,

$$\Delta e_{t,t+k} := \sum_{s=0}^{k-1} \Delta e_{t+s,t+s+1} \frac{100 \cdot N^{top}}{k}.$$

Cumulative returns are averaged over the time horizon k, they are in percentage, and they are multiplied by N^{top}, i.e., the average number of top-days in a year. In our benchmark analysis $N^{top} = 38$.

To ensure that our observations are not influenced by idiosyncratic patterns in our dataset, these averages are computed relative to the average cumulative variation observed in the remaining 85% of business days in our sample. Specifically, we estimate the relative cumulative returns with the following regression:

$$\Delta e^{i,j}_{t,t+k} = a^{i,j}_k + b_k \cdot \mathbb{1}^{Top}_t + \epsilon^{i,j}_{t,k},$$

where $\mathbb{1}^{Top}_t$ is a dummy variable that equals 1 if the day falls in the set of extreme climate news days. b_k captures the relative cumulative returns over a horizon of k days. We only include country pairs where β_i is significantly larger than β_j at 10% level (see figure B.1, Appendix B). Standard errors are clustered at both the date and country-pair level.

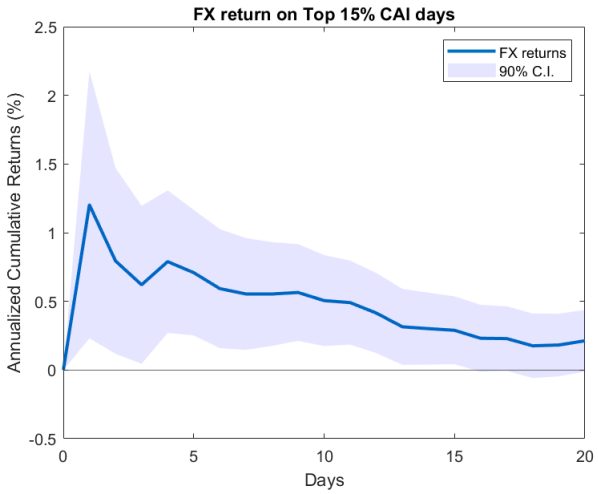


FIG. 7. FX AND INNOVATIONS TO WORLD CLIMATE ATTENTION INDEX (CAI)

Notes: This figure shows the average cumulative return in exchange rates around days with a positive spike (top-15% days in our sample) in the global CAI. This cumulative variation is net of the common cumulative variation that we obtain when considering all other days in our sample. Exchange rates are computed at Greenwich Mean Time in each day across 138 country pairs with exposures to the global CAI that are different from each other at the 10% confidence level. Exchange rates are quoted such that for each country pair an appreciation refers to the country with the higher exposure to global climate news shocks. Our Global Climate Attention Index is based on the methods described in section 3. Countries are equally weighted. The shaded areas present the 90% confidence interval which is constructed using standard errors clustered at both the date and country-pair level.

If climate-related news has no bearing on exchange rates, we would anticipate null cumulative effects. Conversely, our findings reveal that adverse climate news shocks are linked to the contemporaneous appreciation of countries that are comparatively more exposed (i.e., possessing higher β values). Furthermore, this appreciation exhibits persistence and it extends over multiple days, signifying a lasting impact on currencies.

EMs versus DMs. In Figure 8, we illustrate this effect among pairs of countries consisting solely of advanced economies (left panel), developing economies (right panels), or a combination of advanced and developing countries (middle panel).[10] The appreciation pattern is observed across all country pairs. Furthermore, it tends to

[10]We define advanced economies according to the IMF, where the advanced economies in our sample are: AU, CA, CN (HK), FR, DE, IT, JP, KR, NZ, NO, PT, ES, SE, CH, UK, US. The developing economies are: AR, BR, CL, CN, CO, IN, MX, SA, ZA.

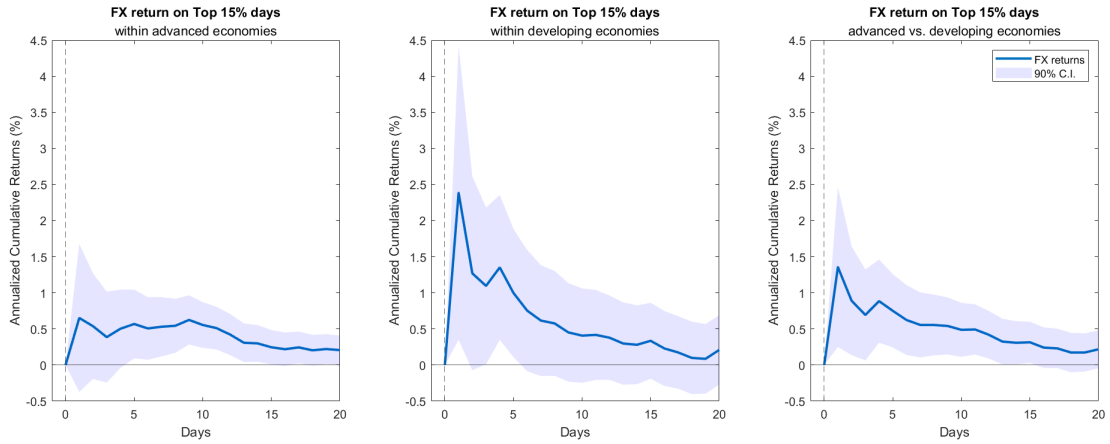


FIG. 8. FX AND INNOVATIONS TO WORLD CAI ACROSS COUNTRY PAIRS

Notes: This figure shows the average cumulative return in exchange rates after days with a top-15% positive spike in the global CAI. For more details, see the notes under figure 7 and section 3. We focus on country pairs in which (i) both countries are advanced economies (left panel), (ii) only one country is defined as an advanced economy (mid panel), and (iii) both countries are developing economies (right panel).

persist longer when at least one emerging country is involved in the analysis.

Type of news. We take advantage of our text analysis results and estimate the following regression:

$$\Delta e^{i,j}_{t,t+k} = a^{i,j}_k + (b_k + c_k \cdot S_t) \cdot \mathbb{1}^{Top}_t + \epsilon^{i,j}_{t,k}, \tag{8}$$

where S_t denotes the share of tweets talking about transition risks at day t, normalized between 0 and 1. This share is computed by using both positive and negative tweets classified as related to transition risk (see figure 6, dark red and dark green shaded areas). In figure 9, we depict the composite coefficient $b_k + c_k \cdot S_t$ for different values of S_t. This specification enables us to identify whether our results are primarily driven by transition of physical risk. We find that the results depicted in figure 7 are consistent with those obtained by estimating equation (8) and setting S_t to its median value. Most importantly, we find that the results are stronger when $S_t = 1$, i.e., in top days when attention is entirely about transition risk.

We repeated this exercise using the share of tweets related to transition risk with a negative sentiment (figure 6, dark red area) and obtained virtually identical results.

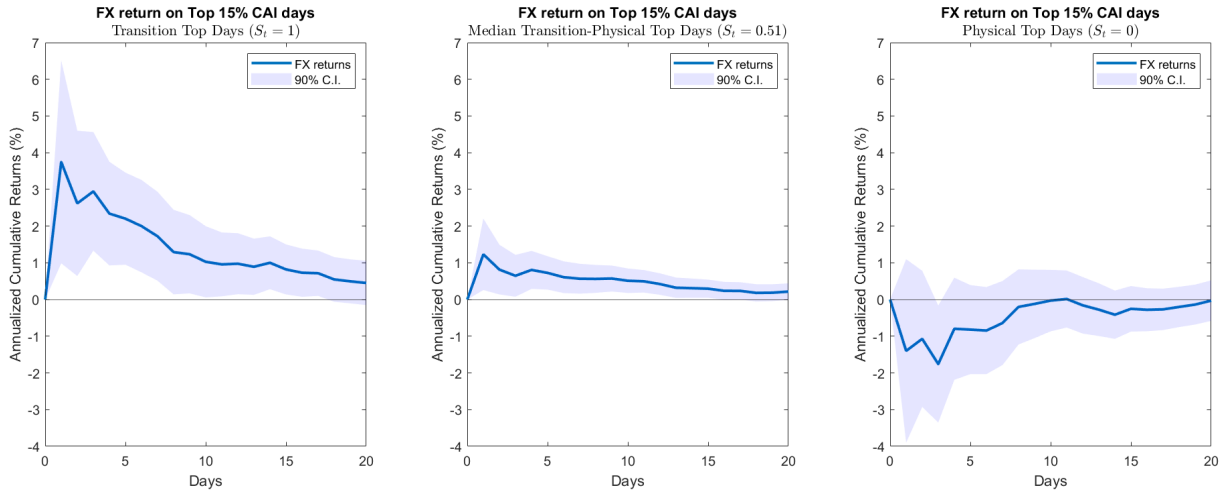


FIG. 9. FX AND WORLD CAI: TRANSITION VS. PHYSICAL DAYS.

Notes: This figures show the average cumulative return in exchange rates after days with a positive spike in the global CAI. The left (right) panel shows the FX responses conditional on the days that the tweets mostly talk about transition risk (equally talk about both physical and transition risk). The specification is

$$\Delta e^{i,j}_{t,t+k} = a^{i,j}_k + (b_k + c_k \cdot S_t) \cdot \mathbb{1}^{Top}_t + \epsilon^{i,j}_{t,k},$$

where S_t denotes the share of tweets talking about transition risks at day t, normalized between 0 and 1. The responses are constructed using the composite coefficient, $b_k + c_k \cdot S_t$, and by choosing different values of S_t.

Even though in the model we do not distinguish between physical and transition climate news, in the data we find that currency appreciation is mostly driven by negative news about transition risk.

4.2 Robustness.

Weighting scheme and top-days threshold. In Appendix B, we show that our results are unchanged when we focus on either a GDP-weighted global index (figure B.2(a)) or a Twitter volume-weighted global index (figure B.2(b)). We also replicate the same exercise by focusing on GDP- and Volume-weighted CAI indeces (figures B.2(a)-B.2(b)). Our results are qualitatively unchanged. In addition, if we change the threshold of top days from 15% to either 10% or 20%, our results remain unchanged (figures B.3(a)-B.3(b)).

Heterogeneity in sensitivity. Figures B.4(a)-B.4(b) confirm that our results are not sensitive to the choice of the significance level that we use in order to select country-pairs with different exposure coefficients. Our results apply regardless of whether we include all country pairs (including those with modest heterogeneity in beta) or just those with a more pronounced degree of heterogeneity (5% confidence level).

The role of the EU. Figure B.5(a) shows that our results are confirmed also when we aggregate the five Euro Area countries in our datatset (DE, FR, IT, PT, ES) into a single entity with a common currency.

Vulnerability. Most importantly, figure B.5(b) confirms that our results are not driven by vulnerability, but rather by the unique information content of our estimated exposure coefficients. Specifically, we orthogonilize our exposure coefficients with respect to vulnerability by considering the residuals of the cross sectional regression depicted in figure 3. The results in figure B.5(b) are based on the residual exposure and are consistent with our benchmark results. Equivalently, using heterogeneity in vulnerability across countries produces insignificant responses. The same conclusions apply to absolute latitude.

Data frequency. Figure B.6(a) confirms our main findings when using exposures estimated at the monthly frequency. Figure B.6(b) is constructed as figure 7 in main text, but it uses weekly observations and it includes weekends. The resulting weekly CAI index covers a total of 430 weeks. During this process, climate-related tweets are aggregated on a weekly basis, with each week of the time series commencing on a Saturday. This weekly aggregation provides a comprehensive perspective on climate-related discussions in social media, encompassing an extended period that includes weekends.[11] Similar to our daily frequency analysis, we identify weeks in which our index records top values and evaluate their cumulative impact on exchange rates.

[11]To identify the top weeks in terms of climate attention, we calculate the growth rate of the weekly global CAI, then the top 10% of observations of this time series are considered as indicative of heightened climate attention. We only keep top weeks that are at least 5 weeks apart to avoid the confounding effects.

Local versus global news. In Figure B.7, we examine local top-attention days, as opposed to global top-attention days. We find that local shocks have no significant impact on FX markets. More broadly, local shocks also appear less relevant in the equity analysis presented next. For brevity, we exclude local shocks from the subsequent analysis.

4.3 Equity returns

Proposition 2 suggests that brown stocks should be more exposed to climate news shocks than green stocks. In addition, this exposure differential should be more pronounced in countries in which sensitivity to climate news is higher (higher b in the model).

Similar to our analysis of currencies, we examine the behavior of average cumulative returns following days marked by a positive spike in our global index (CAI). Consistent with the model, we account for both firm-level "brown-ness"—measured by emission intensity—and country-level sensitivity—captured by our estimated β_i coefficients in Table 2. Emission intensity (defined as tons of CO_2 emissions per unit of sales) is sourced from the Trucost dataset. Our sample includes 16,774 firms, totaling 23,305,563 firm-day observations. Working with such a granular cross section, rather than aggregate country-level equity data, enhances our inference.

Specifically, we estimate the following regression:

$$r^{i,c}_{t,t+k} = \alpha^i_k + \zeta^{i,c}_{t,k} \cdot \mathbb{1}^{Top}_t + \epsilon^{i,c}_{t,k}, \tag{9}$$

$$\zeta^{i,c}_{t,k} = \gamma_{0,k} + (\gamma_{1,k} + \gamma_{2,k} \cdot \beta_c) \cdot E_{i,t_a}, \tag{10}$$

where c denotes the country in which the headquarter of the firm is located, i refers to one of our firms, β_c represents our equally weighted sensitivity, E_{i,t_a} is the emission intensity of firm i assessed the year prior to day t, and $\mathbb{1}^{Top}_t$ is a dummy variable that equals 1 if the day falls in the set of extreme climate news days. In equation (9), the left-hand side variable is defined as follows:

$$r^{i,c}_{t,t+k} = \sum_{s=0}^{k-1} r^{i,c}_{t+s,t+s+1} \frac{100 \cdot N^{top}}{k},$$

that is, it is averaged over the time horizon k, it is in percentage, and it is multiplied by the average number of top-days in a year.

Since emission intensity is very persistent at the annual frequency, the coefficient $\zeta_{t,k}^{i,c}$ is almost time-invariant in our dataset. Consequently, this composite coefficient primarily reflects heterogeneity across different countries and stocks. The literature has proxied the exposure of a firm to climate risk either by examining its emissions or considering geographical factors such as distance from the ocean or latitude.

As in the our model, we hypothesize that a firm's equity returns' sensitivity to climate news reflects the interaction of its brownness and the degree of investor sensitivity to climate news within a specific country. This analysis is agnostic on whether the valuation adjustment is driven by uncertainty about physical damages or transition risk. Given the low correlation between our β_is and vulnerability, we interpret these valuation adjustments as driven mostly by heterogeneous sensitivity to global climate sentiment (discount rate channel).

According to our model, global climate news should play an important role mostly among firms with high emissions in highly sensitive countries ($\gamma_{2,k} < 0$). Our estimates confirm this prediction. In figure 10, we depict the estimates of our composite parameter $\hat{\zeta}_{t,k}^{i,c}$ over different daily horizons, k.

In the top portion of the figure, we first sort countries according to their exposure β. The top-decile of the distribution of βs is 2.27 (Saudi Arabia). The bottom-decile is 0.197 (South Africa). We then select the values of carbon emission intensity for a representative green (brown) firm using the 5th (95th) percentile of the emission intensity distribution, which corresponds to the median value within the top-decile (bottom-decile).[12] Given these numbers, we can depict the implied estimated composite coefficient $\zeta_{t,k}^{i,c}$ and its associated standard error across different daily horizons, k.

The bottom two panels convey the same information as the top panels but from a different perspective. Specifically, the bottom left (right) panel presents the composite coefficients for a representative green (brown) firm in a low-β country and in a high-β country.

[12]The 5th (95th) percentile of the log emission intensity in our sample is 0.43 (6.88). The thresholds remain consistent both across and within countries because the country-level distribution of emission intensities is stable. See figure B.8 in the appendix for more details.

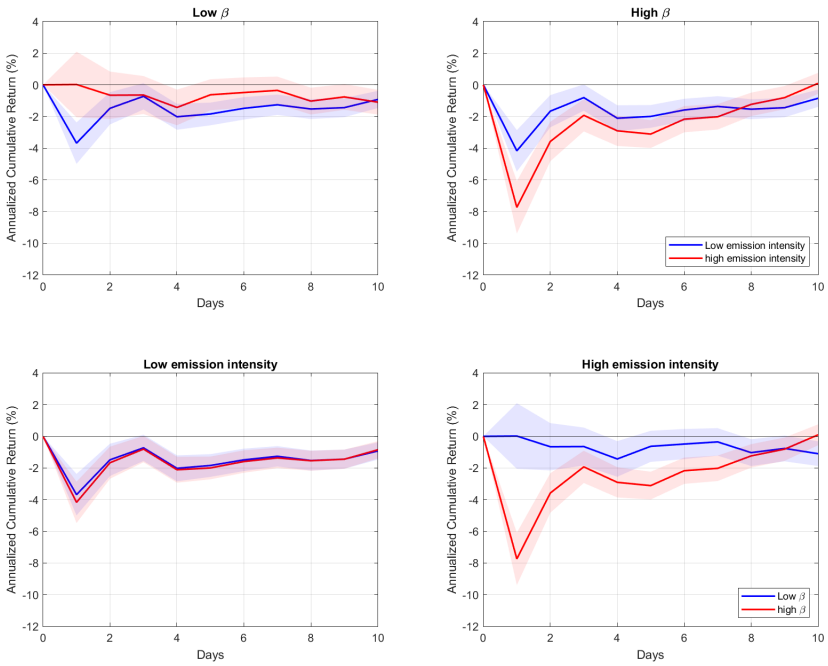


FIG. 10. USD EQUITY RETURNS AND INNOVATIONS TO WORLD CAI

Notes: This figure shows the average cumulative return in equity returns after days with a top-15% positive spike in the global CAI. For more details, see the notes under figure 7. We depict the estimates of $\zeta_{t,k}^{i,c}$ as defined in equations (9)-(10) across different daily horizons, k. Standard errors are clustered at the industry×date and firm level. We follow the Fama-French 49 classification. The sample comprises a total of about 23 million firm-day observations. Daily returns are annualizedusing the average number of top climate days in a year. In the four panels, high (low) β refers to the top-decile (bottom-decile) of betas across countries in our sample, and high (low) emission intensity is using the top- and bottom-5% of emission-sorted firms in our sample. The shaded areas present the 90% confidence interval.

Our analysis yields several significant findings. Firstly, firms situated in countries with moderate sensitivity to climate sentiment news experience a more moderate loss of value. This effect holds for both high- and low-emission firms. Conversely, firms in countries with high β values suffer a more severe loss of value, an effect that is particularly pronounced for high-emission firms. Across all these scenarios, the negative impact on cumulative returns is very persistent.

Changing the order of the sorting variables does not alter our conclusions. Specifically, the bottom two panels of figure 10 confirm that firms located in 'naturally hedged' countries (that is, countries with low β) are generally less affected by ad-

verse climate sentiment news. However, when examining stocks with high emission intensity, the negative impact on valuation is more severe for firms in countries with a higher climate news sensitivity, β.

Type of news. Following our analysis of currency markets, we examine whether these results are primarily driven by top-attention days in which news focuses on either physical or transition risk. Specifically, we estimate the following specification:

$$\begin{aligned} r^{i,c}_{t,t+k} &= \alpha^i_k + \zeta^{i,c}_{t,k} \cdot 1^{Top}_t + \epsilon^{i,c}_{t,k}, \\ \zeta^{i,c}_{t,k} &= (\gamma_{0,k} + (\gamma_{1,k} + \gamma_{2,k} \cdot \beta_c) \cdot E_{i,t_a}) + (\kappa_{0,k} + (\kappa_{1,k} + \kappa_{2,k} \cdot \beta_c) \cdot E_{i,t_a}) \cdot S_t, \end{aligned}$$

where S_t represents the share of tweets discussing transition risks on day t, normalized between 0 and 1. Figure B.10 in the appendix presents our results. The responses are constructed using the composite coefficient $\zeta^{i,c}_{t,k}$, with $S_t = 0.50$ in the left panel and $S_t = 1$ in the right panel. For a median top-attention day, this specification reproduces the results reported in Figure 10. When news is primarily about transition risk, we observe more pronounced depreciations across all panels. As with currency markets, equity depreciations are largely driven by negative news on transition risk. When we focus exclusively on the share of transition-related tweets with negative sentiment, the results are amplified by a factor of two.

Robustness. In Appendix B, we show that our results are robust across various methodological changes. Panel (a) in Figure B.9 uses GDP-weighted CAI, while Panel (b) employs Twitter Volume-weighted CAI. Both panels confirm the robustness of our findings as documented in Figure 10. Furthermore, Figure B.11 compares the response of equity returns using thresholds of 10% and 20% to identify spikes in CAI, respectively. This figure documents that our results remain qualitatively unchanged regardless of the chosen threshold.

Figure B.12 provides supplementary analyses to validate our findings. In Panel (a) we cluster standard errors at the country×industry×date and firm levels, while in Panel (b) we use residual βs obtained by regressing our exposure coefficients on the University of Notre Dame's vulnerability index. These results corroborate our main conclusions.

Most importantly, our results are not solely driven by the exchange rate adjustment. As shown in figure B.13, our results hold also when we focus on returns expressed in local currency.

5 International Flows

In this section, we test the prediction of our Proposition 3, that is, the current account of countries with higher climate sensitivity should decline when adverse sentiment news materialize. In the data, we are interested in estimating the following system of equations:

$$\Delta CAI_{i,t} = \beta_i \cdot \overline{\Delta CAI}_t + u_{i,t} \tag{11}$$

$$\begin{aligned} \Delta\left(\frac{NX_{i,t}}{GDP_{i,t}}\right) - \Delta\left(\frac{NX_{j,t}}{GDP_{j,t}}\right) &= \Gamma \cdot (\beta_i - \beta_j)\, \overline{\Delta CAI}_t + ... \\ &\quad + \theta' \cdot (control_{i,t} - control_{j,t}) + \epsilon_{ij,t}, \end{aligned} \tag{12}$$

where $\frac{NX_{i,t}}{GDP_{i,t}}$ is the net export over GDP of country i at time t. We add the first difference to make sure that all variables are stationary. $\Delta CAI_{i,t}$ denotes the growth rate of the climate attention index for country i and quarter t, $\overline{\Delta CAI}_t$ is the cross-sectional average of ΔCAI_t at date t, i.e., the global CAI index.[13] The term $control$ is a vector of control variables including the change in the industrial production index (ΔIPI), to control for country-specific productivity shocks, and the share of Twitter volume on days when the CAI is at the bottom 5%, to control for other events that affect Twitter activities. In the appendix, we consider a more general version of our model which features also local climate news shocks with volatility σ_z. In main text, we abstract away from local shocks by setting $\sigma_z = 0$ because in our international setting global shocks feature a prominent role.

We provide results based on the cases in which $\overline{\Delta CAI}_t$ is constructed in one of three ways: (i) by equally weighting all countries, (ii) by weighting each country proportion-

[13] In order to eliminate the effect of the Covid-19 and the beginning of the war in Ukraine, we have regressed $\Delta CAI_{i,t}$ on two dummies of 2020Q2 and 2022Q1 for each country, and obtain the residual for our analysis.

ally to its share of global GDP, and (iii) by weighting each country proportionally to its share of Twitter volumes.

Simple OLS on both equations will produce incorrect inference for the coefficient Γ, because the β coefficients in equation (12) are themselves estimated from equation (11). We address this econometric issue by estimating the system via GMM with a pre-determined weighting matrix. Specifically, the set of moment conditions is

$$g_T(\beta,\gamma,\theta) = E_T\begin{bmatrix} u_{i,t}\overline{\Delta CAI}_t \\ \epsilon_{ij,t}\left(\beta_i-\beta_j\right)\overline{\Delta CAI}_t \\ \epsilon_{ij,t}\left(control_{i,t}-control_{j,t}\right)\end{bmatrix} = E_T\begin{bmatrix} g_1(\beta) \\ g_2(\beta,\Gamma,\theta)\end{bmatrix}$$

where $g_1(\beta)$ is the vector of orthogonality conditions associated to equation (11) for each country i, and $g_2(\beta,\Gamma,\theta)$ stacks the three orthogonality conditions associated to equation (12) for each country pair $\{i,j\}$. The first block g_1 pins down β, and the second block g_2 pins down the remaining coefficients Γ,θ. Given two control variables, if we have N countries in our sample, the number of moments will be $N+2N\times(N-1)$, and the number of parameters is $N+4$. This is an over-identified GMM problem for $N>2$.

Next, we follow Cochrane (2009) and estimate the following linear combination of the moment conditions:

$$a_T g_T = 0$$

where

$$a_T = \begin{bmatrix} I_N & 0 \\ 0 & \frac{\partial g_2(\beta,\gamma,\theta)}{\partial[\gamma,\theta]}W\end{bmatrix}$$

with I_N and W being identity matrices of size N and $2N\times(N-1)$, respectively. Weighting the block of orthogonality conditions of equation 11 with an identity matrix ensures that the estimated vector of βs coincides with OLS estimates. The set of moments conditions in g_2 is instead efficiently estimated. Denote by $b=[\beta,\gamma,\theta]'$ the vector of all parameters. The asymptotic distribution of b is given by

$$\sqrt{T}(\hat{b}-b)\sim N\left(0,(ad)^{-1}aSa'(ad)'^{-1}\right)$$

where $a=\lim_{T\to\infty}a_T$, $d=\frac{\partial g_t}{\partial b}$ is the gradient, and S is the spectral density matrix estimated using the residuals.

Given our interest on the role of global climate news shocks on the dynamics of international trade, we focus on the estimated parameter Γ in equation (12). According to our model, this coefficient should be negative. We estimate the parameters of interest using an expanding window to show whether the estimated coefficient is stable over different sample periods. Specifically, we fix our starting period at 2015:Q1 (where our sample begins), and expand the end of sample from 2016:Q4 to 2022:Q4. The estimated Γ coefficient along with its 90% confidence interval are presented in figure 11.

Our estimates support the prediction of our model, as they suggest that an adverse global climate shock produces an outflow of resources away from countries with a lower exposure. This result is confirmed across different ways to aggregate our country-level CAI in order to form a global index. In addition, our result is driven mainly by country pairs in which there is at least one developed economy. This is broadly consistent with the spirit of our model since we assume that risk sharing is implemented with frictionless trade. We show that these effects on the current account can persist for six months (see Figure B.14 in the appendix).

6 Concluding Remarks

Our research significantly contributes to our understanding of the impact of global climate attention on economic and financial outcomes. The availability of high frequency data is particularly valuable as it enables a more direct analysis of how climate news shocks reverberate throughout global financial markets and influence currencies on a global scale. The establishment of a clear connection between climate attention shocks and bilateral trade among nations represents a noteworthy advancement for both the macro-finance literature and policymakers.

Moreover, the economic model we introduce, along with the climate attention index we propose, open up various avenues for future research. For instance, our economic theory implies that heightened global news attention to climate issues may influence decisions regarding investments in green technology. Furthermore, the climate attention index we have developed can be leveraged to explore the relationship between climate-related news and returns on a wide range of assets above and beyond

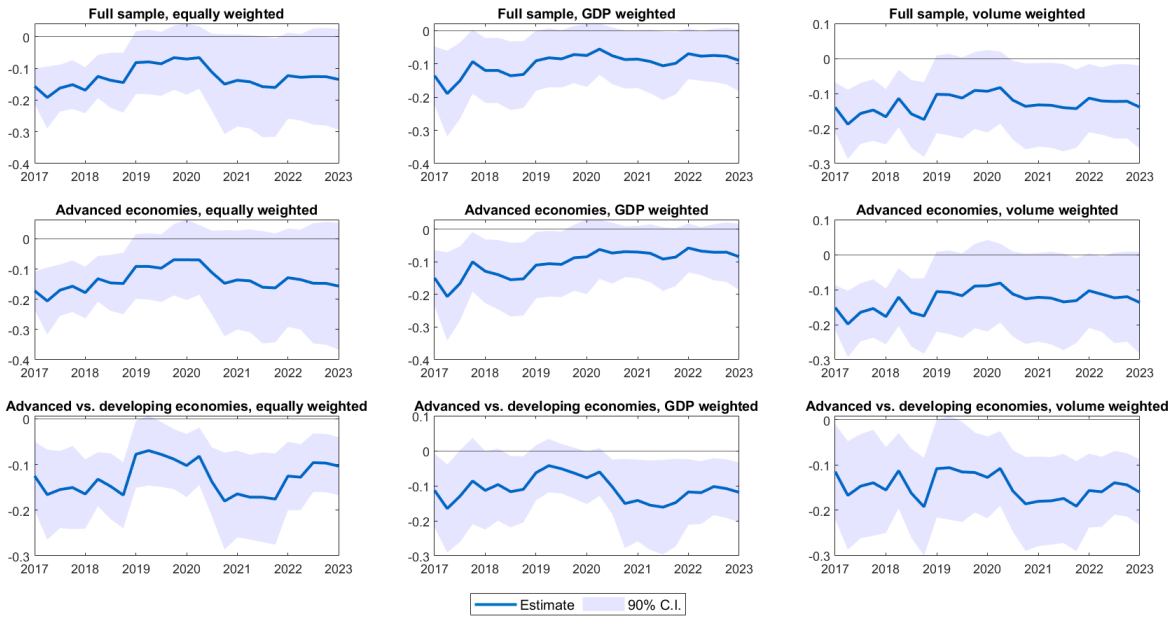


FIG. 11. GMM ESTIMATION OF Γ.

Notes: The figure shows estimates of Γ (defined in equation (12)) using expanding time windows. Each window starts in 2015:Q1 and ends on the date reported on the x-axis. The parameter Γ is estimated using the GMM described in section 2. Panels in different columns refer to results obtained from different ways to aggregate country-level CAI indices in order to form a global component. Panels in different rows refer to results obtained from different groups of country-pairs. Advanced economies are defined according to the IMF. Standard errors are HAC-adjusted. The shaded areas present the 90% confidence interval.

stocks, both within individual countries and across international borders. These potential research directions hold promise for gaining deeper insights into the complex interplay between climate awareness and economic and financial dynamics.

Establishing a connection between attention to climate news and currency movements is of paramount importance in the current global landscape. As climate change becomes an increasingly pressing concern, understanding how shifts in climate attention impact financial markets and trade can inform both economic policies and investment strategies. It provides a valuable tool for policymakers to anticipate and respond to economic implications of climate-related events and offers investors insights into the potential risks and opportunities associated with climate awareness. By shedding light on these intricate connections, our research serves not only the academic community but also contributes to the broader efforts to address the multifaceted challenges posed by climate change on a global scale.

References

Acharya, V. V., T. Johnson, S. Sundaresan, and T. Tomunen. Is physical climate risk priced? evidence from regional variation in exposure to heat stress. Technical Report w30445 National Bureau of Economic Research 2022 https://www.nber.org/papers/w30445.

Albuquerque, R., M. S. Kruttli, Y. Ma, and S. W. Watugala. Financing and the green paradox. Working Paper March 2025.

Backus, D. K., P. J. Kehoe, and F. E. Kydland. 1994. Dynamics of the trade balance and the terms of trade: The J-curve? American Economic Review 84(1):84–103.

Baker, S. R., N. Bloom, and S. J. Davis. 2016. Measuring economic policy uncertainty*. The Quarterly Journal of Economics 131(4):1593.

Bansal, R., D. Kiku, and M. Ochoa. Climate change risk. Technical report Federal Reserve Bank of San Francisco 2019 https://www.frbsf.org/economic-research/events/2019/november/economics-of-climate-change/files/Paper-5-2019-11-8-Kiku-1PM-1st-paper.pdf.

Barbieri, F., L. Espinosa Anke, and J. Camacho-Collados. XLM-T: Multilingual language models in Twitter for sentiment analysis and beyond. In Proceedings of the Thirteenth Language Resources and Evaluation Conference. European Language Resources Association 06 2022.

Bolton, P., and M. Kacperczyk. 2021. Do investors care about carbon risk? Journal of Financial Economics 142(2):517–549. doi: 10.1016/j.jfineco.2021.05.008.

Bolton, P., and M. Kacperczyk. 2023. Global pricing of carbon-transition risk. Journal of Finance 78(6):3677–3754. doi: 10.1111/jofi.13272.

Bolton, P., M. T. Kacperczyk, and M. Wiedemann. The co2 question: Technical progress and the climate crisis. Technical report Working Paper 2023 https://ssrn.com/abstract=4212567.

Cochrane, J. Asset pricing: Revised edition. Princeton university press 2009.

Colacito, R., M. Croce, S. Ho, and P. Howard. November 2018. Bkk the ez way: International long-run growth news and capital flows. American Economic Review 108(11):3416–49.

Colacito, R., B. Hoffmann, and T. Phan. 2019. Temperature and growth: A panel analysis of the united states. Journal of Money, Credit and Banking 51(2-3):313–368. doi: https://doi.org/10.1111/jmcb.12574.

Della Corte, P., L. Sarno, and I. Tsiakas. 2009. An Economic Evaluation of Empirical Exchange Rate Models. Review of Financial Studies 22(9):2491–530.

Della Corte, P., L. Sarno, and I. Tsiakas. 2011. Spot and forward volatility in foreign exchange. Journal of Financial Economics 100(3):496 – 513.

Della Corte, P., T. Ramadorai, and L. Sarno. 2016. Volatility risk premia and exchange rate predictability. Journal of Financial Economics 120(1):21 – 40. ISSN 0304-405X.

Engle, R. F., S. Giglio, B. Kelly, H. Lee, and J. Stroebel. 2020. Hedging Climate Change News. The Review of Financial Studies 33(3).

Giglio, S., B. Kelly, and J. Stroebel. 2021a. Climate finance. Annual Review of Financial Economics 13:15–36. doi: 10.1146/annurev-financial-102620-103311.

Giglio, S., M. Maggiori, K. Rao, J. Stroebel, and A. Weber. 2021b. Climate change and long-run discount rates: Evidence from real estate. The Review of Financial Studies 34(8):3527–3571. doi: 10.1093/rfs/hhab032.

Giglio, S., T. Kuchler, J. Stroebel, and X. Zeng. Biodiversity risk. Technical Report w31137 National Bureau of Economic Research 2023 https://www.nber.org/papers/w31137.

Grootendorst, M. 2022. Bertopic: Neural topic modeling with a class-based tf-idf procedure. arXiv preprint arXiv:2203.05794.

Hassan, T. 2013. Country size, currency unions, and international asset returns. The Journal of Finance 68:2269–308.

Hassan, T., T. Mertens, and T. Zhang. 2015. Currency manipulation. Working Paper.

Hassan, T. A., T. M. Mertens, and T. Zhang. 2016. Not so disconnected: Exchange rates and the capital stock. Journal of International Economics 99:S43–S57.

Hassan, T. A., S. Hollander, L. Van Lent, and A. Tahoun. 2019. Firm-level political risk: Measurement and effects. The Quarterly Journal of Economics 134(4):2135–2202.

Hassan, T. A., J. Schreger, M. Schwedeler, and A. Tahoun. 2023. Sources and Transmission of Country Risk. The Review of Economic Studies. ISSN 0034-6527.

Hsu, P.-h., K. Li, and C.-y. Tsou. 2023. The pollution premium. The Journal of Finance 78(3): 1343–1392.

Ivanov, I. T., M. S. Kruttli, and S. W. Watugala. 2024. Banking on carbon: Corporate lending and cap-and-trade policy. The Review of Financial Studies 37(5):1640–1684. doi: 10.1093/rfs/hhad085.

Javadi, S., A.-A. Masum, M. Aram, and R. P. Rao. 2023. Climate change and corporate cash holdings: Global evidence. Financial Management 52(2):253–295.

Jung, H., R. Engle, S. Ge, and X. Zeng. Physical climate risk factors and an application to measuring insurers' climate risk exposure. Staff Report 1066 Federal Reserve Bank of New York July 2023.

Kashyap, A., N. Kovrijnykh, and A. Pavlova. 2024. Designing esg benchmarks. Working paper.

Kruttli, M. S., B. Roth Tran, and S. W. Watugala. January 2025. Pricing poseidon: Extreme weather uncertainty and firm return dynamics. The Journal of Finance.

Lee, S. O., N. C. Mark, J. Nauerz, J. Rawls, and Z. Wei. 2022. Global temperature shocks and real exchange rates. Journal of Climate Finance 1:100004.

Leombroni, M., A. Vedolin, G. Venter, and P. Whelan. 2021. Central bank communication and the yield curve. Journal of Financial Economics 141(3). ISSN 0304-405X.

Lustig, H., N. Roussanov, and A. Verdelhan. 2011. Common risk factors in currency markets. Review of Financial Studies 24:3731–77.

Lustig, H., N. Roussanov, and A. Verdelhan. 2014. Countercyclical currency risk premia. Journal of Financial Economics 111(3):527–553.

Mueller, P., A. Stathopoulos, and A. Vedolin. 2017. International correlation risk. Journal of Financial Economics.

Pástor, L., R. F. Stambaugh, and L. A. Taylor. 2021. Sustainable investing in equilibrium. Journal of Financial Economics 142(2):550–571. doi: 10.1016/j.jfineco.2020.12.011.

Pástor, L., R. F. Stambaugh, and L. A. Taylor. 2022. Dissecting green returns. Journal of Financial Economics 146(2):403–424. doi: 10.1016/j.jfineco.2022.07.007.

Pavlova, A., and R. Rigobon. 2007. Asset prices and exchange rates. Review of Financial Studies 20:1139–1181.

Pavlova, A., and R. Rigobon. 2010. An asset-pricing view of external adjustment. Journal of International Economics 80:144–156.

Pavlova, A., and R. Rigobon. 2013. International macro-finance. Handbook of Safeguarding Global Financial Stability: Political, Social, Cultural, and Economic Theories and Models 2: 169–176.

Reimers, N., and I. Gurevych. Sentence-bert: Sentence embeddings using siamese bert-networks. In Proceedings of the 2019 Conference on Empirical Methods in Natural Language Processing. Association for Computational Linguistics 11 2019.

Sandulescu, M., F. Trojani, and A. Vedolin. 2020. Model-free international stochastic discount factors. Journal of Finance. forthcoming.

Sautner, Z., L. Van Lent, G. Vilkov, and R. Zhang. 2023. Firm-Level Climate Change Exposure. Journal of Finance.

Shi, Z., and S. Zhang. Oil and greenium. Working Paper, May 2025 2025.

Starks, L. T. 2023. Presidential address: Sustainable finance and esg issues – value versus values. Journal of Finance 78:1837–1872. doi: 10.1111/jofi.13255.

Webersinke, N., M. Kraus, J. Bingler, and M. Leippold. ClimateBERT: A Pretrained Language Model for Climate-Related Text. In Proceedings of AAAI 2022 Fall Symposium: The Role of AI in Responding to Climate Challenges 2022. doi: https://doi.org/10.48550/arXiv.2212.13631.

Zhang, S. 2024. Carbon returns across the globe. The Journal of Finance. Forthcoming.

Zviadadze, I. 2017. Term structure of consumption risk premia in the cross section of currency returns. Journal of Finance.

Internet Appendix

Appendix A. Data collection

TABLE A.1: Newspaper Twitter Handles by Country

Country	Newspaper name	Twitter handle	Language
Argentina	Clarín	clarincom	Spanish
	Diario Crónica	cronica	
	Infobae	infobae	
	La Nación	LANACION	
Australia	The Australian	australian	English
	The Daily Telegraph	dailytelegraph	
	The Australian Financial Review	FinancialReview	
	The Age	theage	
Brazil	Estadão	Estadao	Portuguese
	Folha de S.Paulo	folha	
	GauchaZH	GauchaZH	
	Jornal O Globo	JornalOGlobo	
Canada	The Globe and Mail	globeandmail	English
	Montreal Gazette	mtlgazette	
	Ottawa Citizen	OttawaCitizen	
	Toronto Star	TorontoStar	
	The Vancouver Sun	VancouverSun	
Switzerland	20 Minuten	20min	German
	24 heures	24heuresch	
	Le Temps	LeTemps	French
	Neue Zürcher Zeitung	NZZ	
Chile	El Mercurio	ElMercurio_cl	Spanish
	El Mostrador	elmostrador	
	La Tercera	latercera	
China	China Daily	ChinaDaily	English
	People's Daily China	PDChina	
	China Xinhua News	XHNews	
Colombia	El Colombiano	elcolombiano	Spanish
	El Espectador	elespectador	
	El Heraldo Colombia	elheraldoco	
Germany	BILD	BILD	German
	Frankfurter Allgemeine	faznet	
	Handelsblatt	handelsblatt	
	ZEIT ONLINE	zeitonline	
Spain	ABC	abc_es	Spanish
	El País	el_pais	
	El Mundo	elmundoes	
	La Vanguardia	LaVanguardia	
France	Le Figaro	Le_Figaro	French
	Le Parisien	le_Parisien	
	Le Monde	lemondefr	
	Libération	libe	
China (Hong Kong)	Hong Kong Free Press	HongKongFP	English
	RTHK News	rthk_enews	

Country	Newspaper name	Twitter handle	Language
	SCMP News	SCMPNews	
India	Economic Times Hindustan Times The Hindu Times of India	EconomicTimes htTweets the_hindu timesofindia	English
Italy	Corriere della Sera Repubblica Il Sole 24 ORE	Corriere repubblica sole24ore	Italian
Japan	Asahi Shimbun AJW The Japan Times Japan Today The Japan News	AJWasahi japantimes JapanToday The_Japan_News	English
Korea	The Korea JoongAng Daily The Korea Times The Korea Herald Yonhap News	JoongAngDaily koreatimescokr TheKoreaHerald YonhapNews	English
Mexico	El Universal La Jornada Milenio Reforma	El_Universal_Mx lajornadaonline Milenio Reforma	Spanish
Norway	Aftenposten Dagbladet VG	Aftenposten dagbladet vgnett	Norwegian
New Zealand	Dominion Post ODT - Otago Daily Times The Press Newsroom	DomPost odtnews PressNewsroom	English
Portugal	Correio da Manhã Expresso Jornal de Notícias	cmjornal expresso JornalNoticias	Portuguese
Saudi Arabia	Al Jazirah Alwatan OKAZ	al_jazirah AlwatanSA OKAZ_online	Arabic
Sweden	Dagens Nyheter Goteborgs Posten Svenska Dagbladet Sydsvenskan	dagensnyheter GoteborgsPosten SvD sydsvenskan	Swedish
United Kingdom	BBC News Financial Times The Guardian The Times and The Sunday Times	BBCNews FinancialTimes guardiannews thetimes	English
United States	Boston Globe Chicago Tribune Dallas News Houston Chronicle LA Times Miami Herald NY Times SF Chronicle USA Today	BostonGlobe chicagotribune dallasnews HoustonChron latimes MiamiHerald nytimes sfchronicle USATODAY	English

Country	Newspaper name	Twitter handle	Language
	Washinton Post	washingtonpost	
	Wall Street Journal	WSJ	
South Africa	Daily Sun	dailysunsa	English
	Sunday Times	SundayTimesZA	
	Times Live	TimesLIVE	

Notes: This table lists the official Twitter handles of major national newspapers across 30 countries, along with their names and publication languages. The information spans the period 2014–2022 and serves as the basis for constructing our climate attention indices using social media data.

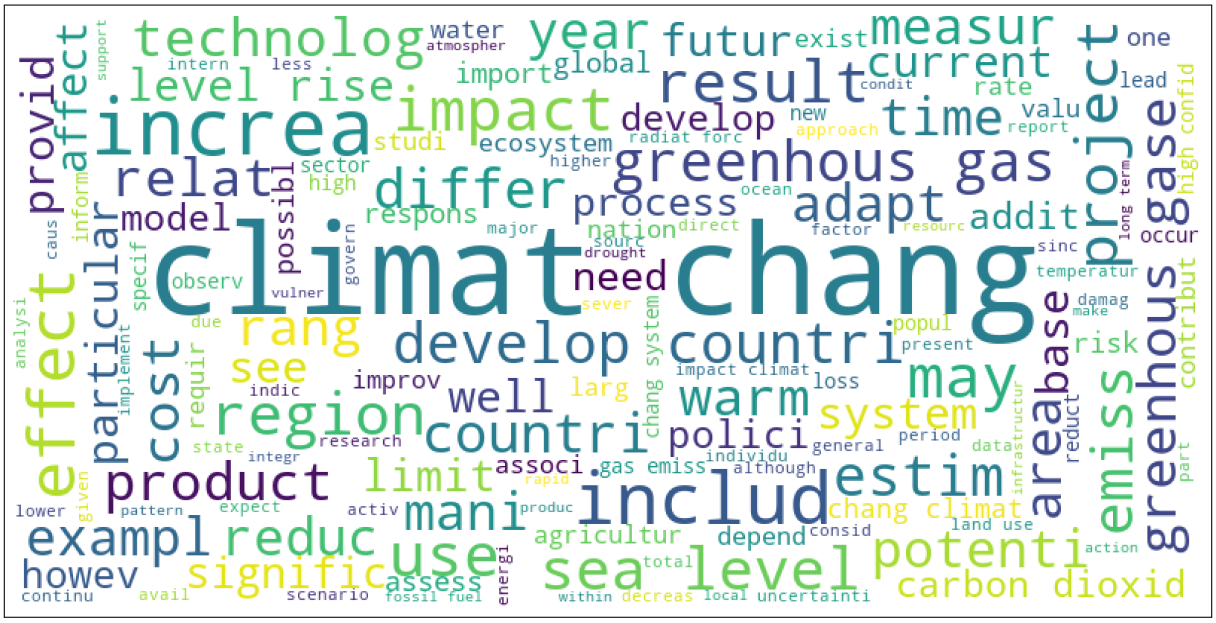


FIG. A.1. WORD CLOUD FOR THE PRE-PROCESSED CORPUS

Notes: This figure shows the cloud of the word roots of authoritative texts used in the construction of the Climate Attention Index. See Engle et al. (2020). Our preprocess: (1) removes any special characters and/or numbers, (2) removes stop words (e.g, "and" "or"), (3) stems each word (using the Snowball algorithm), and (4) keeps only words with more than two characters. We translated this corpus to different languages to build an index for non-English speaking countries.

TABLE A.2. AI-GENERATED SENTENCES

	Physical Risk	Transition Risk
1	Hurricanes are becoming more intense	New carbon taxes increase energy costs
2	Rising sea levels threaten coastal cities	Governments are enforcing stricter emission limits
3	Wildfires are spreading faster each year	Climate policies impact fossil fuel investments
4	Floods are more frequent in urban areas	Carbon pricing is affecting industry competitiveness
5	Droughts are lasting longer worldwide	Environmental regulations are tightening worldwide
6	Heatwaves are breaking records globally	Firms must comply with stricter sustainability laws
7	Cyclones are forming earlier than expected	Carbon offsets are becoming a mandatory requirement
8	Tornadoes are appearing in new regions	Subsidies for renewable energy are rising
9	Storm surges endanger coastal communities	Stricter reporting rules affect corporate disclosures
10	Melting glaciers contribute to rising seas	Regulatory risks impact financial markets
11	Arctic ice is melting at record speeds	Fossil fuel demand is declining
12	Permafrost is thawing, releasing methane	Renewable energy adoption is accelerating
13	Global temperatures are steadily increasing	Investors are divesting from coal industries
14	Extreme cold events are less frequent	Gas prices fluctuate due to energy transitions
15	Ocean temperatures are rising rapidly	Green bonds are reshaping capital markets
16	Coral reefs are dying due to warming seas	The electric vehicle market is expanding rapidly
17	Changing seasons affect crop production	Oil companies face increasing financial pressure
18	More frequent heatwaves strain electricity grids	Hydrogen energy is gaining policy support
19	Polar vortex disruptions cause unusual cold	Nuclear power investments are rising
20	Snowfall patterns are shifting globally	Battery storage is critical for renewable energy growth
21	Rivers are drying up due to prolonged droughts	Energy efficiency technologies are reshaping industries
22	Flash floods destroy homes and roads	Carbon capture projects are scaling up
23	Drinking water sources are shrinking	Solar power efficiency is improving rapidly
24	Groundwater levels are depleting	Wind farms are replacing coal plants
25	Heavy rainfall increases landslide risks	Smart grids are enabling decentralized energy systems
26	Freshwater lakes are shrinking worldwide	Climate-friendly materials are replacing traditional ones
27	Ice sheets are collapsing faster than expected	Green hydrogen is becoming more viable
28	Saltwater intrusion threatens freshwater supplies	Electrification of transportation is accelerating
29	Dams are failing under extreme weather	Sustainable agriculture technologies are emerging
30	Reservoirs are running dry in many regions	Circular economy practices are gaining traction
31	Desertification is expanding in dry regions	Lawsuits against polluting companies are increasing
32	Livestock suffers from water shortages	Investors are demanding climate risk disclosures
33	Pests spread as temperatures rise	Regulators require firms to report climate risks
34	Changing climates affect coffee production	Non-compliance with emissions laws leads to penalties
35	Soil erosion worsens with heavy rain	Litigation risks threaten fossil fuel companies
36	Crop yields are declining due to heat stress	Banks must assess climate risks in lending portfolios
37	Unpredictable rainfall disrupts farming	Corporate climate pledges face legal scrutiny
38	Fisheries collapse due to warming oceans	Greenwashing claims lead to reputational damage
39	Extreme weather damages food supply chains	Disclosure failures result in investor lawsuits
40	More frequent frost events harm fruit crops	Companies face pressure to adopt net-zero targets
41	Roads crack under extreme heat	Job losses in fossil fuel industries are rising
42	Floods overwhelm drainage systems	Green jobs are reshaping the labor market
43	Airports close due to extreme weather	Energy prices are volatile due to policy shifts
44	Power outages increase with heatwaves	Consumer preferences are shifting toward sustainability
45	Rising insurance costs strain homeowners	Supply chains are adapting to climate policies
46	Heat damages rail tracks and highways	Financial institutions are reassessing climate risks
47	Coastal erosion threatens real estate	Insurance premiums rise due to climate-related policies
48	Ports are closing due to severe storms	Carbon-intensive industries face declining revenues
49	Cold snaps increase energy demand	Developing economies struggle with climate transition costs
50	Business disruptions rise with climate events	Global trade patterns are shifting due to decarbonization

Notes: This table shows sentences randomly generated by ChatGPT about climate physical and transition risk.

Appendix B. Additional Empirical Results

Significance of climate attention βs. Figure B.1 depicts the values of the t-stat used to test the following null assumption $H_0 : \beta_i - \beta_j = 0, i \neq j$ for all possible country pairs in our dataset. The test is based on a joint estimation of equation (7) for each possible pair of country i and j. Dark colors refer to values of the t-stat with an associated confidence level smaller than 10%. We depict the country-pair test results only in the bottom portion of the figure because the upper portion is symmetric.

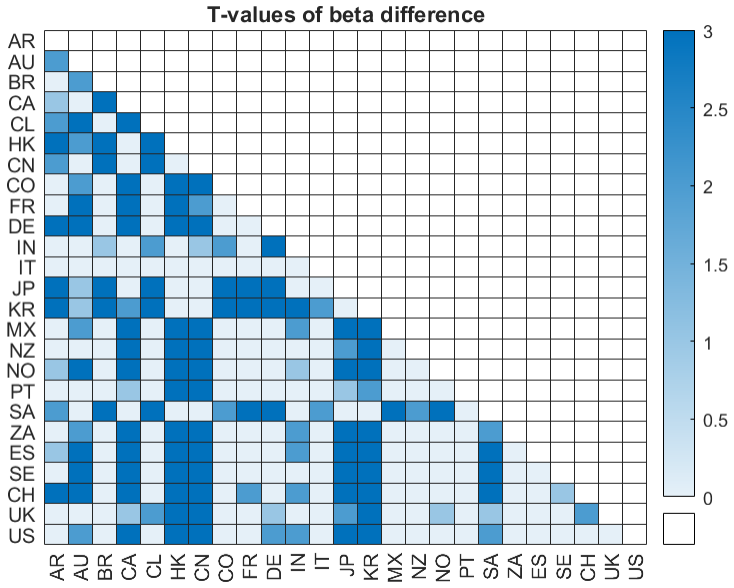


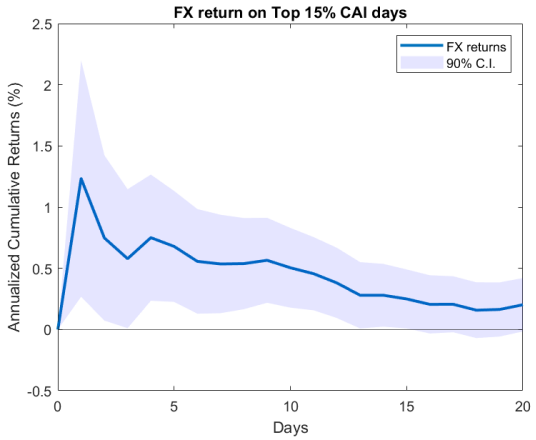
FIG. B.1. HETEROGENEOUS EXPOSURES ACROSS COUNTRY PAIRS

Notes: This figure shows the values of the t-stat used to test the following null assumption $H_0 : \beta_i - \beta_j = 0, i \neq j$ for all possible country pairs in our dataset. The test is based on a joint estimation of equation (7) for each possible pair of country i and j. Dark colors refer to values of the t-stat with an associated confidence level smaller than 10%. We depict the country-pair test results only in the bottom portion of the figure because the upper portion is symmetric.

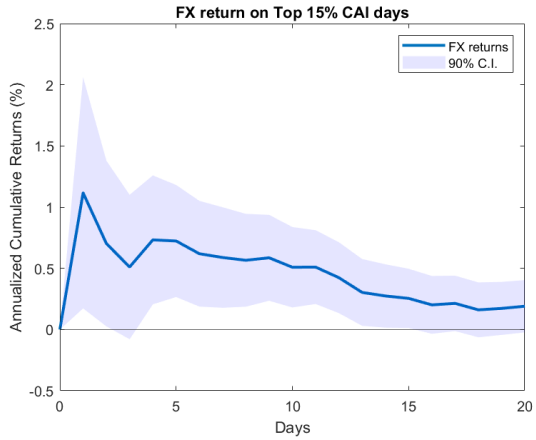
Robustness of FX response. Figures B.2(a)-B.2(b) are constructed as figure 7 reported in main text, except that we compute our global CAI by weighting our countries by their GDP and tweets volume, respectively.

In figures B.3(a)-B.3(b) we consider top-10% and top-20% days, respectively. Our results are not sensitive to the percentile that we choose.

Figures B.4(a)-B.4(b) confirm that our results are not sensitive to the choice of the signif-



B.2(a) GDP-Weighted



B.2(b) Volume-Weighted

FIG. B.2. FX AND WORLD CAI: THE ROLE OF THE WEIGHTING SCHEME.

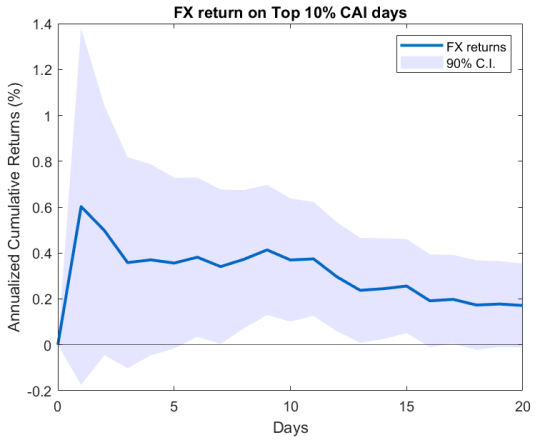
Notes: average cumulative return in exchange rates after days with a positive spike in the global CAI. Panel A is constructed as figure 7 except that country exposures are obtained by regressing country-level CAI on the GDP-weighted global CAI. Panel B is constructed as figure 7 except that country exposures are obtained by regressing country-level CAI on the Twitter Volume-weighted global CAI.

icance level that we use in order to select country-pairs with different exposure coefficients. Our results apply regardless of whether we include all country pairs (including those with modest heterogeneity in beta) or just those with a more pronounced degree of heterogeneity (5% confidence level).

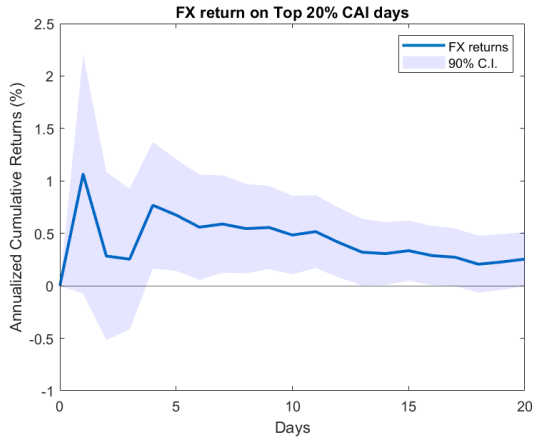
Figure B.5(a) shows that our results are confirmed also when we aggregate five Euro Area countries in our datatset (DE, FR, IT, PT, ES) in just one entity with one currency. Most importantly, figure B.5(b) confirms that our results are not driven by vulnerability, but rather by the unique information content of our estimated esposure coefficients.

Figure B.6(a) confirms our main findings when using exposures estimated at the monthly frequency. Figure B.6(b) is constructed as figure 7 in main text, but it uses weekly observations and it includes weekends. Figure 9 shows that our results are mainly driven by days in which the news are predominantly about transition risk.

Robustness of the equity analysis. Figure B.8 illustrates the distribution of emission intensity across firms, segmented by country. Emission intensity is calculated as the ratio of tons of CO2 emissions to sales, derived from the Trucost dataset. The dataset includes 16,774 firms, providing a comprehensive overview of country-level emission profiles.



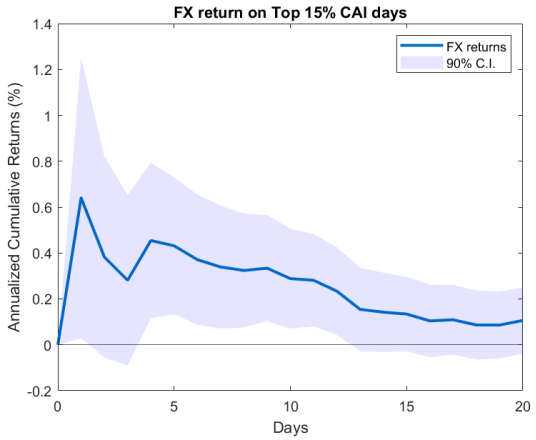
B.3(a) Top 10% Days



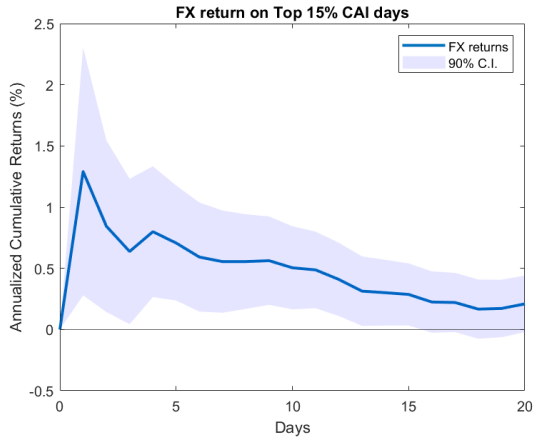
B.3(b) Top 20% Days

FIG. B.3. FX AND WORLD CAI: THE ROLE OF THE THRESHOLD.

Notes: average cumulative return in exchange rates around days with a positive spike in the global CAI. Panel A selects the top CAI days according to a top-10% threshold, while Panel B selects the top CAI days according to a top-20% threshold. For more details, see the notes under figure 7.



B.4(a) All Country Pairs

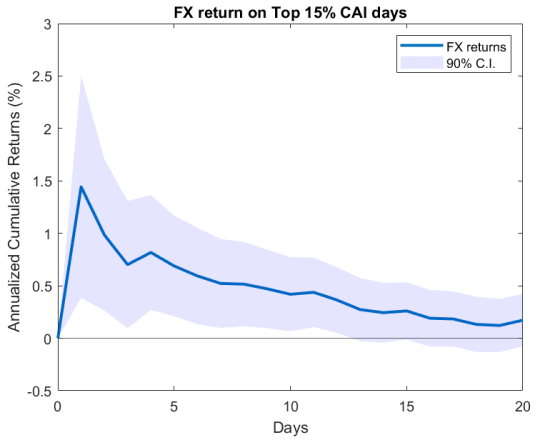


B.4(b) β Different at 5%

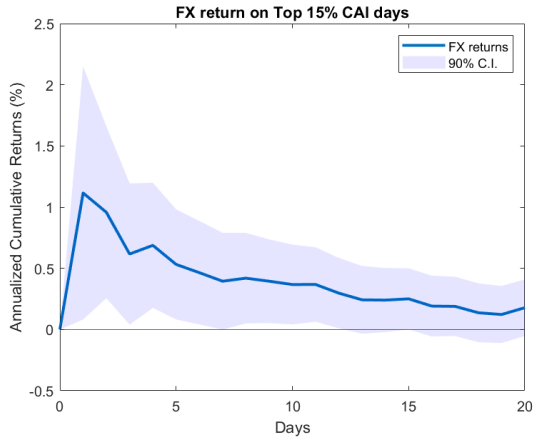
FIG. B.4. FX AND WORLD CAI: THE ROLE OF β.

Notes: average cumulative return in FX rates after days with a positive spike in global CAI. Panel A uses all 300 country pairs. Panel B selects country pairs such that their betas are significantly different at least at the 5% confidence level. For more details, see the notes under figure 7.

Figure B.9 examines the relationship between equity returns and the global Climate Action Index (CAI) using different weighting methods. Panel (a) uses GDP-weighted global CAI



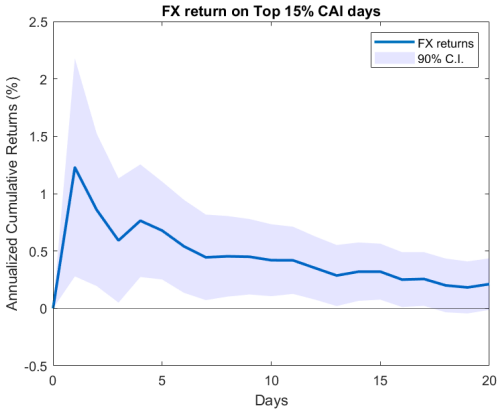
B.5(a) Combine EU



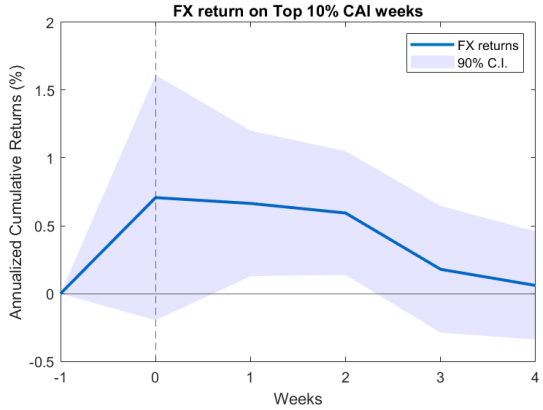
B.5(b) Residual Betas

FIG. B.5. FX AND WORLD CAI: ADDITIONAL ROBUSTNESS.

Notes: Panel (a) shows the average cumulative return in FX rates after days with a positive spike in the global CAI, combining the five EU countries (DE, FR, IT, PT, ES) by averaging their β exposures. Panel (b) uses the residual component of country exposures after regressing on the vulnerability index from the University of Notre Dame to repeat the analysis. See notes to figure 7 for details.



B.6(a) Monthly Data



B.6(b) Weekly Data

FIG. B.6. FX AND INNOVATIONS TO WORLD CAI: FREQUENCY ANALYSIS.

Notes: Panel (a) shows the average cumulative return in exchange rates after days with a positive spike in the global CAI, using monthly data to estimate country exposures instead of quarterly data. Panel (b) shows the average cumulative return after weeks with a positive spike in the global CAI, considering all 300 country pairs and selecting the top-10% weeks. To avoid confounding effects, weeks are chosen so that they do not overlap over a 5-week window. See notes to figure 7 for details.

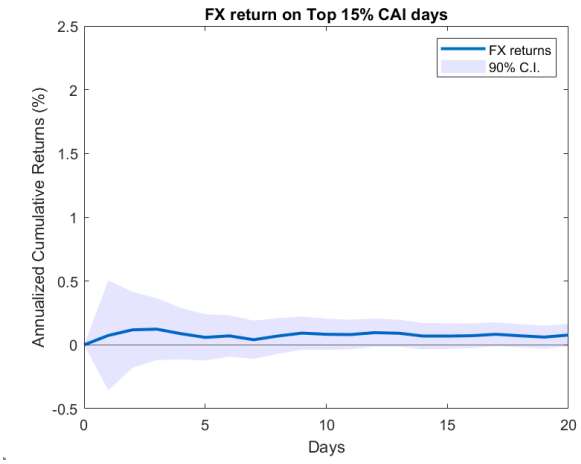


FIG. B.7. FX AND INNOVATIONS TO LOCAL CAI.

Notes: This figure shows the average cumulative return in exchange rates after days with a positive spike in the local CAI, defined as the residual from regressing a country's CAI on the global CAI. Specifically, we estimate

$$\Delta e^{i,j}_{t,t+k} = a^{i,j}_k + b_k \cdot \left(\mathbb{1}^{Top}_{i,t} - \mathbb{1}^{Top}_{j,t}\right) + \epsilon^{i,j}_{t,k},$$

For each country i, the local top-day dummy $\mathbb{1}^{Top}_{i,t}$ is based on the top-15% days of the country's local CAI. See notes to figure 7 for more details.

to estimate country exposures, while Panel (b) employs Twitter Volume-weighted global CAI. These results are consistent with the analysis presented in the main text (Figure 10), highlighting the robustness of the findings to weighting schemes.

Figure B.11 compares equity returns following days with large positive spikes in the global CAI. Panel (a) focuses on the top-10% of positive spikes, and Panel (b) examines the top-20% of positive spikes. The results align with those reported in the main text (Figure 10), confirming the robustness of the findings of our analysis.

Figure B.12 presents supplementary analyses on equity returns and the global CAI. Panel (a) incorporates clustered standard errors at the country×industry×date and firm level, while Panel (b) uses residual betas derived from regressions of exposure coefficients on the University of Notre Dame's vulnerability index. These findings are consistent with the main text (Figure 10) and provide further validation of the results under alternative methodological specifications.

Figure B.13 presents supplementary analyses on equity returns expressed in local currency.

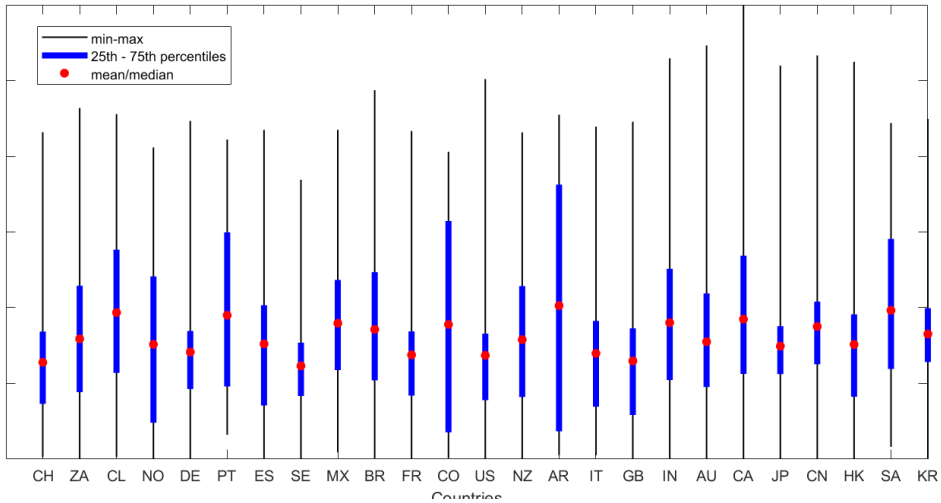
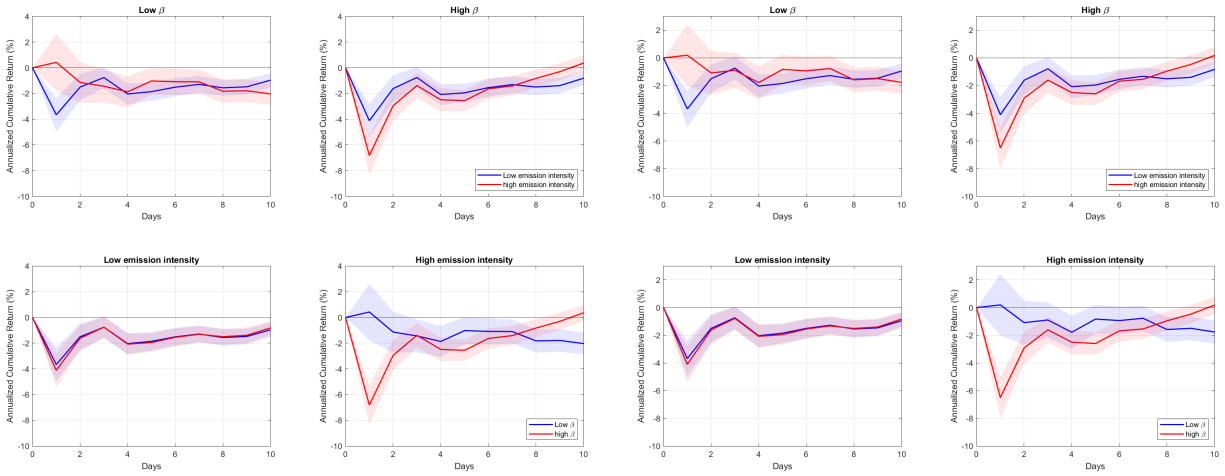


FIG. B.8. EMISSION INTENSITY BY COUNTRY

Notes: This figure shows distribution of emission intensity across firms by country. Emission intensity is computed as tons of CO2 divided by sales and it is obtained from the Trucost dataset. We have a total of 16,774 firms.

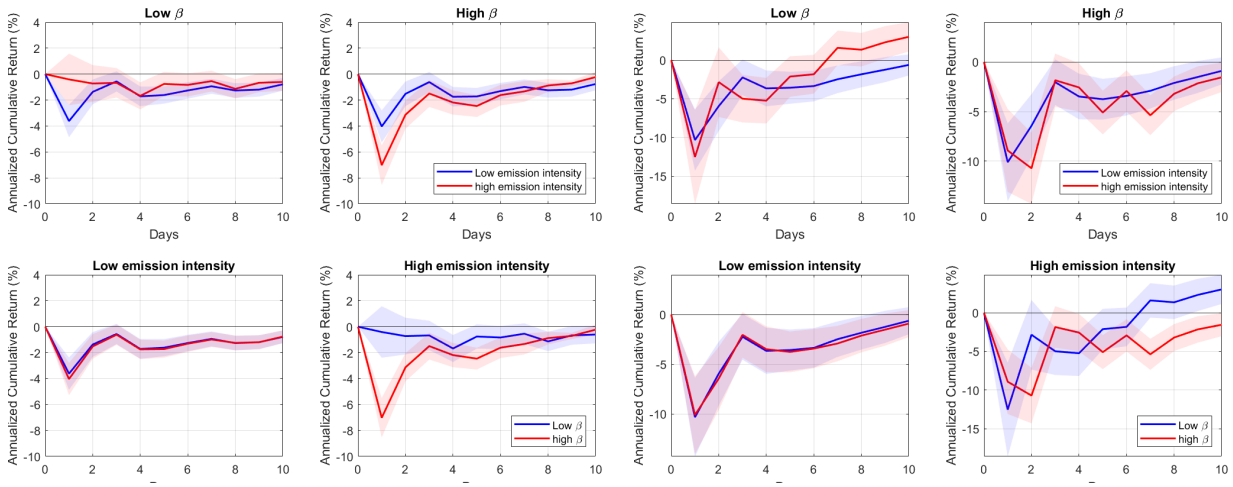


B.9(a) GDP-Weighted

B.9(b) Volume-Weighted

FIG. B.9. EQUITY RETURNS AND WORLD CAI: THE ROLE OF WEIGHTING.

Notes: Panel (a) shows the average cumulative return in equity returns after days with a top-15% positive spike in the global CAI, using the GDP-weighted global CAI to estimate country exposures. Panel (b) shows the results when using the Twitter Volume-weighted global CAI for the same estimation. For more details, see the notes under figure 10.



B.10(a) Median Transition/Physical Top Days

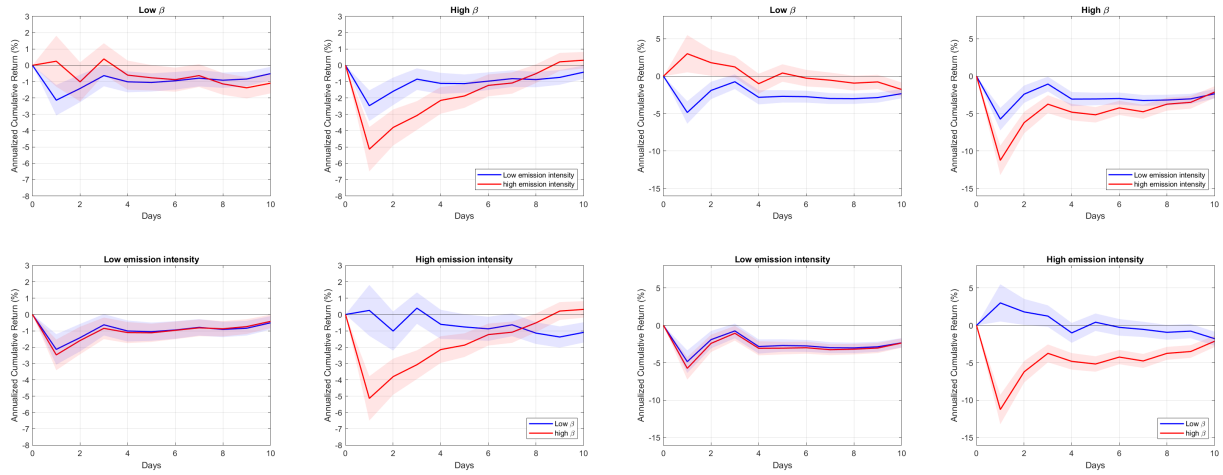
B.10(b) Transition Top Days

FIG. B.10. EQUITY AND WORLD CAI: TRANSITION VS. PHYSICAL DAYS.

Notes: This figure shows the average cumulative return in equity returns after days with a top-15% positive spike in the global CAI, Panel (a) and (b) show the equity return responses conditional on the share of daily tweets related to transition risk being equal to 50% and 100%, respectively. We estimate the following specification

$$\begin{aligned} r^{i,c}_{t,t+k} &= \alpha^i_k + \beta^{i,c}_{t,k} \cdot 1^{Top}_t + \epsilon^{i,c}_{t,k}, \\ \beta^{i,c}_{t,k} &= (\gamma_{0,k} + (\gamma_{1,k} + \gamma_{2,k} \cdot \beta_c) \cdot E_{i,t_a}) + (\kappa_{0,k} + (\kappa_{1,k} + \kappa_{2,k} \cdot \beta_c) \cdot E_{i,t_a}) \cdot S_t, \end{aligned}$$

where S_t denotes the share of tweets talking about transition risks at day t, normalized between 0 and 1. The responses are constructed using the composite coefficient, $\beta^{i,c}_{t,k}$, and by setting $S_t = 0.50$ and $S_t = 1$. For more details, see the notes under figure 10.

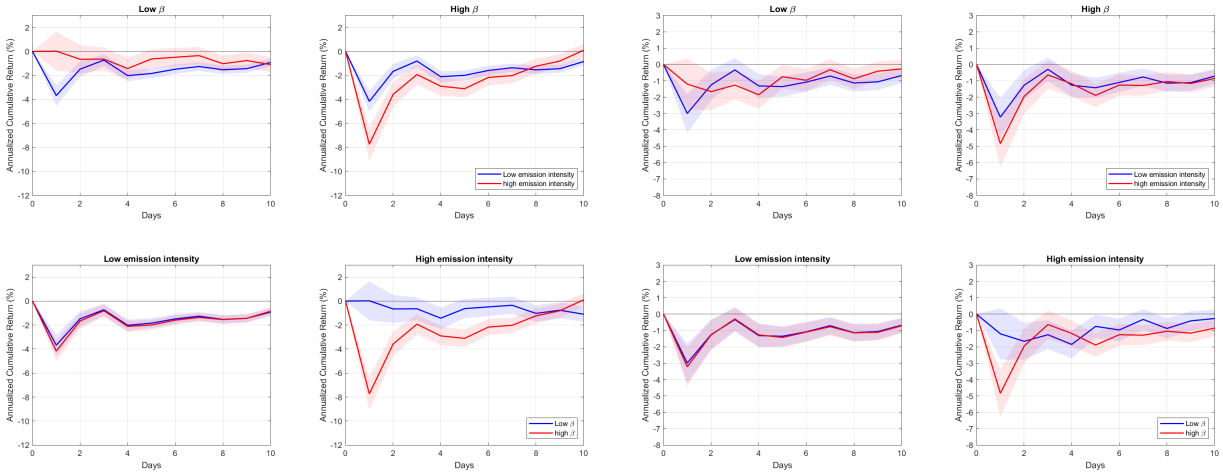


B.11(a) Top 10% Days

B.11(b) Top 20% Days

FIG. B.11. EQUITY RETURNS AND WORLD CAI: TOP 10% VS. TOP 20% DAYS.

Notes: Panel (a) shows the average cumulative return in equity returns after days with a top-10% positive spike in the global CAI. Panel (b) shows the results for days with a top-20% positive spike in the global CAI. For more details, see the notes under figure 10.



B.12(a) Clustered Standard Errors

B.12(b) Residual Betas

FIG. B.12. EQUITY RETURNS AND WORLD CAI: ADDITIONAL RESULTS.

Notes: Panel (a) shows the average cumulative return in equity returns after days with a top-15% positive spike in the global CAI, clustering standard errors at the country×industry×date and firm level. Panel (b) shows the results when using residual betas obtained by regressing the exposure coefficients on the vulnerability index from the University of Notre Dame. For more details, see the notes under figure 10.

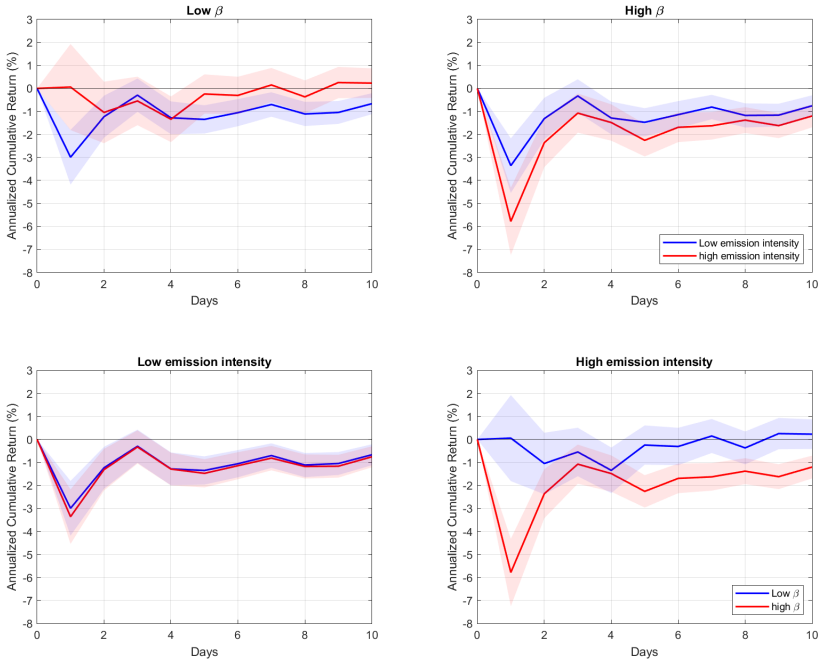


FIG. B.13. LOCAL EQUITY RETURNS AND INNOVATIONS TO WORLD CAI

Notes: This figure shows the average cumulative return in equity returns after days with a top-15% positive spike in the global CAI. Returns are in local units (as opposed to USD) and in percentage. For more details, see the notes under figure 10.

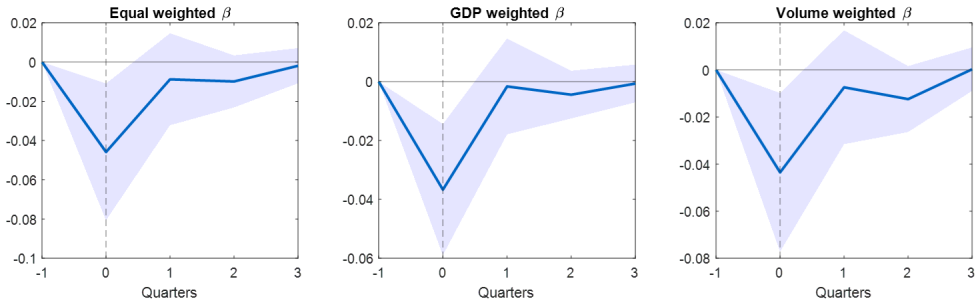


FIG. B.14. GMM ESTIMATION OF Γ OVER DIFFERENT HORIZONS.

Notes: The figure shows estimates of Γ using the following quarterly regression specification for $k = 0, 1, 2, 3$,

$$\frac{1}{k+1}\left[\Delta\left(\frac{NX}{GDP}\right)_{i,t-1\to t+k} - \Delta\left(\frac{NX}{GDP}\right)_{j,t-1\to t+k}\right] = \alpha^{ij} + \Gamma\overline{\Delta CAI}_t + \theta(control_i - control_j) + \epsilon_t^{ij}$$

We include and order country pairs such that $\beta_i > \beta_j$. Panels in different columns refer to results obtained from different ways to aggregate country-level CAI indices in order to form a global component. *control* include the changes in the industrial production and Twitter volume at bottom 5% CAI days. Standard errors are HAC-adjusted and clustered at the quarter. The shaded areas present the 90% confidence interval.

Appendix C. Model

In this section, we present both the full description and key derivations of our model. For a more detailed analysis of international models of risk-sharing with recursive preferences and news shows, see Colacito et al. (2018).

C.1 Setup

We generalize the two-period setting presented in Colacito et al. (2018) to include: (i) green investment, (ii) disutility from climate shocks, and (iii) climate sentiment shocks. We assume that the intertemporal elasticity of substitution (henceforth IES) is equal to 1 and the preferences are defined as

$$u_t = (1-\beta)\log\left(\widetilde{C}_t \cdot \mathcal{G}_t\right) + \frac{\beta}{1-\gamma}\log E_t\left[\exp\left\{(1-\gamma)u_{t+1}\right\}\right], \quad t = \{0,1,2\},$$

where $\mathcal{G}_t$ captures climate-related sentiment shocks, includes both a standard consumption bundle C_t and an endogenous disruption term $\tilde{D}_t$: $\widetilde{C}_t = C_t \cdot \tilde{D}_t^{-1}$. The sentiment process evolves as $\mathcal{G}_t = e^{-b \cdot g_t}$, where g_t is a zero-mean normally distributed global climate news shock. In what follows, we derive all equilibrium conditions using an equivalent formulation of the model:

$$u_t = (1-\beta)\log\left(C_t D_t^{-a}\right) + \frac{\beta}{1-\gamma}\log E_t\left[\exp\left\{u_{t+1}(1-\gamma)\right\}\right],$$

where $D_t = \mathcal{G}_t \cdot \tilde{D}_t$. At time $t = 1$, two news shocks, $\theta \sim N(0, \sigma_\theta^2)$ and $\tilde{g} \sim N(0, \sigma_g^2)$, occur. The shock θ determines the productivity of capital at $t = 2$, whereas $\tilde{g} > 0$ is a bad shock to climate sentiment. At time $t = 1$, uncertainty is resolved and utilities of the home and foreign country are

$$u_1 = (1-\beta)\log\left(C_1 D_1^{-a}\right) + \tilde{\beta}\log\left(C_2 D_2^{-a}\right), \qquad u_1^* = (1-\beta)\log\left(C_1^* D_1^{*-a}\right) + \tilde{\beta}\log\left(C_2^* D_2^{*-a}\right), \tag{C.1}$$

where $\tilde{\beta} = \beta(1-\beta)$ and

$$C_t = X_t^{\lambda} Y_t^{(1-\lambda)}, \quad C_t^* = X_t^{*(1-\lambda)} Y_t^{*\lambda}, \forall t = \{1,2\}$$

denote the consumption bundles, the parameter $a \in (0,1)$ captures the disutility from climate-related damage, and D_t is the amount of damage times the sentiment shock. The damage depends on both aggregate output and green investment. At time $t = 1$, D_1 and D_1^* are given, while D_2 and D_2^* denote the composite climate-related damages at time $t = 2$ in the home and

foreign countries, respectively. Specifically:

$$D_2 = e^{b\tilde{g}} \left(e^{\theta} B/I_g\right)^{\lambda_g} \left(e^{-\theta} B^*/I_g^*\right)^{1-\lambda_g}, \quad D_2^* = e^{\tilde{g}} \left(e^{-\theta} B^*/I_g^*\right)^{\lambda_g} \left(e^{\theta} B/I_g\right)^{1-\lambda_g},$$

where b captures the sensitivity of the home country to global climate news (the exposure of foreign country is normalized to unity), λ_g captures the home bias in climate-related damage; B and B^* are aggregation of time $t = 1$ investment for the home and foreign countries and are defined as

$$B = I_{x,1}^{\lambda_I} I_{x,1}^{*1-\lambda_I}, \quad B^* = I_{y,1}^{1-\lambda_I} I_{y,1}^{*\lambda_I}. \tag{C.2}$$

Note that, since all uncertainty is resolved at time $t = 1$, the above formulation is mathematically equivalent to the one in the main text, where g is modeled as a time-1 sentiment shock. The two settings are identical provided that $g \sim N(0, (a\sigma_g/\beta)^2)$, or equivalently, $g = \frac{a}{\beta}\tilde{g}$.
Time $t = 2$ output in the two countries is determined as $e^{\theta}B$ and $e^{-\theta}B^*$. The economy-wide resource constraints are

$$1 = X_1 + X_1^* + I_{x,1} + I_{y,1} + I_g, \qquad 1 = Y_1 + Y_1^* + I_{y,1}^* + I_{x,1}^* + I_g^*$$
$$e^{\theta}B = X_2 + X_2^*, \qquad e^{-\theta}B^* = Y_2 + Y_2^*.$$

Throughout this Appendix, we retain the following assumption on the domain of the parameters.

Assumption C1. *Assume home bias in consumption, investment, and cliamte-related damage, that is,* $0.5 < \lambda, \lambda_I, \lambda_g < 1$. *In addition, assume* $\frac{1-a}{2} < \hat{\lambda} = \lambda - a\lambda_g < 1 - a$ *(home bias in the consumption-damage composite).*

Social planner problem and pseudo Pareto weights. The social planner chooses allocations of consumption goods $\{X_t, X_t^*, Y_t, Y_t^*\}_{t=1,2}$, and allocations of investments $I_{x,1}$, $I_{y,1}$, I_g, $I_{y,1}^*$, $I_{x,1}^*$, I_g^* to maximize

$$W = \mu_0 E_0[u_1] + (1 - \mu_0) E_0[u_1^*],$$

where μ_0 and $(1 - \mu_0)$ denote the date $t = 0$ Pareto weights attached to the two agents. Define $\widetilde{S}_0 := \frac{\mu_0}{1-\mu_0}$ and let $\widetilde{S}_1$ be the ratio of pseudo-Pareto weights after the news shocks are realized. Colacito et al. (2018) show that:

$$\widetilde{S}_1 = \widetilde{S}_0 \exp\left\{(u_1 - u_1^*)(1 - \gamma)\right\}.$$

If we initialize the economy under the assumption that the distribution of wealth at date $t = 0$ is identical across the two countries, then

$$\widetilde{s}_1 := \log \widetilde{S}_1 = (u_1 - u_1^*)(1 - \gamma). \tag{C.3}$$

In what follows, we document that the solutions for u_1 and u_1^* are linear in the time $t = 1$ shocks, θ and g. It follows that the solution for $\widetilde{s}_1$ is also linear:

$$\widetilde{s}_1 = \lambda_s^\theta \cdot \theta + \lambda_s^g \cdot g, \tag{C.4}$$

where the coefficients λ_s^θ and λ_s^g are determined in equilibrium. Finally, since all uncertainty is resolved at time $t = 1$, we have $\widetilde{S}_2 = \widetilde{S}_1$.

C.2 Solution of the Model

Since the model features a finite horizon, we begin the analysis by solving the terminal period and proceed recursively backward.

Time 2. The optimization problem at time $t = 2$ is

$$\begin{aligned} \max_{X_2, X_2^*, Y_2, Y_2^*} \quad & \widetilde{S}_2 u_2 + u_2^* \\ s.t. \quad & e^\theta B = X_2 + X_2^*, \quad e^{-\theta} B^* = Y_2 + Y_2^*. \end{aligned}$$

Note that the objective function can be written as

$$\widetilde{S}_2 \left(\lambda \log X_2 + (1-\lambda) \log Y_2 - a \log D_2\right) + \left((1-\lambda) \log X_2^* + \lambda \log Y_2^* - a \log D_2^*\right).$$

The optimal condition is

$$\frac{\widetilde{S}_2 \lambda}{X_2} = \frac{1-\lambda}{X_2^*}, \quad \frac{\widetilde{S}_2 (1-\lambda)}{Y_2} = \frac{\lambda}{Y_2^*}.$$

Using the condition that $\widetilde{S}_2 = \widetilde{S}_1$, the solution for the home country is

$$X_2 = \frac{\lambda \widetilde{S}_1}{1 - \lambda + \lambda \widetilde{S}_1} e^\theta B, \quad Y_2 = \frac{(1-\lambda)\widetilde{S}_1}{\lambda + (1-\lambda)\widetilde{S}_1} e^{-\theta} B^*.$$

The solution for foreign country follows by symmetry. We can log-linearize this solution around $\bar{s} = 0$ (which means, equal initial size of the two countries, i.e., zero net foreign asset

position) to obtain

$$\log X_2 \approx \log\lambda + (1-\lambda)\widetilde{s}_1 + \theta + \log B, \quad \log Y_2 \approx \log(1-\lambda) + \lambda\widetilde{s}_1 - \theta + \log B^*.$$

It follows that:

$$\begin{aligned} \log C_2 D_2^{-a} &= const + (2\lambda-1)\theta + 2\lambda(1-\lambda)\widetilde{s}_1 + \lambda\log B + (1-\lambda)\log B^* - a\log D_2 \quad \text{(C.5)} \\ \log C_2^* D_2^{*-a} &= const - (2\lambda-1)\theta - 2\lambda(1-\lambda)\widetilde{s}_1 + (1-\lambda)\log B + \lambda\log B^* - a\log D_2^* \end{aligned}$$

where

$$\begin{aligned} \log D_2 &= \lambda_g(\log B - \log I_g + \theta) + (1-\lambda_g)(\log B^* - \log I_g^* - \theta) + bg \quad \text{(C.6)} \\ \log D_2^* &= \lambda_g(\log B^* - \log I_g^* - \theta) + (1-\lambda_g)(\log B - \log I_g + \theta) + g, \quad \text{(C.7)} \end{aligned}$$

respectively.

Time 1. At time $t=1$, the social planner chooses the allocations of consumption goods, X_1, X_1^*, Y_1, Y_1^*, of investment goods in the brown technology, $I_{x,1}$, $I_{y,1}$, $I_{y,1}^*$, $I_{x,1}^*$, and investment goods in the green technology, I_g, I_g^* to maximize

$$\widetilde{S}_1\left(\log C_1 + \beta\log C_2 D_2^{-a}\right) + \left(\log C_1^* + \beta\log C_2^* D_2^{*-a}\right) \quad \text{(C.8)}$$

subject to the two economy-wide feasibility constraints:

$$1 = X_1 + X_1^* + I_{x,1} + I_{y,1} + I_g, \qquad 1 = Y_1 + Y_1^* + I_{y,1}^* + I_{x,1}^* + I_g^*, \quad \text{(C.9)}$$

Since we set $D_1 = D_1^* = 1$ and $(1-\beta)$ is a multiplicative coefficient of the objective function, we can omit them from this maximazation. Using the time $t=2$ equilibrium solutions for $\log\left(C_2 D_2^{-a}\right)$ and $\log\left(C_2^* D_2^{*-a}\right)$ in (C.5), the definitions of $\log(D_2)$ and $\log(\log D_2^*)$ in (C.6), and the definitions of B and $B*$ in (C.2), we can expand the objective function in (C.8) as

$$\begin{aligned} &\widetilde{S}_1\Big\{\lambda\log X_1 + (1-\lambda)\log Y_1 + \beta\Big[(2\lambda-1)\theta + 2\lambda(1-\lambda)\widetilde{s}_1 + \hat{\lambda}\left(\lambda_I\log I_{x,1} + (1-\lambda_I)I_{x,1}^*\right) \quad \text{(C.10)} \\ &+(1-a-\hat{\lambda})\left(\lambda_I\log I_{y,1}^* + (1-\lambda_I)\log I_{y,1}\right) - a\left[-\lambda_g\log I_g - (1-\lambda_g)\log I_g^* + (2\lambda_g-1)\theta + bg\right]\Big]\Big\} \\ &+\lambda\log Y_1^* + (1-\lambda)\log X_1^* + \beta\Big[-(2\lambda-1)\theta - 2\lambda(1-\lambda)\widetilde{s}_1 + (1-a-\hat{\lambda})\left(\lambda_I\log I_{x,1} + (1-\lambda_I)I_{x,1}^*\right) \\ &+\hat{\lambda}\left(\lambda_I\log I_{y,1}^* + (1-\lambda_I)\log I_{y,1}\right) - a\left[-\lambda_g\log I_g^* - (1-\lambda_g)\log I_g - (2\lambda_g-1)\theta + g\right]\Big], \end{aligned}$$

where $\hat{\lambda} \equiv \lambda - a\lambda_g$. Since the economy-wide feasibility constraints in (C.9) are linear in the choice variables, we can use them to express I_g and I_g^* as functions of the remaining choice variables. Substituting these expressions into the objective function (C.10) yields the following solution from the first-order necessary conditions:

1. Consumption goods:

$$X_1 = \frac{1}{K}\widetilde{S}_1\lambda, \quad X_1^* = \frac{1}{K}(1-\lambda), \quad Y_1^* = \frac{1}{K^*}\lambda, \quad Y_1 = \frac{1}{K^*}\widetilde{S}_1(1-\lambda)$$

2. Investments in the brown technology:

$$I_{x,1} = \frac{\beta\lambda_I}{K}\left(\widetilde{S}_1\hat{\lambda} + 1 - a - \hat{\lambda}\right), \quad I_{y,1} = \frac{\beta(1-\lambda_I)}{K}\left(\widetilde{S}_1(1-a-\hat{\lambda}) + \hat{\lambda}\right),$$
$$I_{y,1}^* = \frac{\beta\lambda_I}{K^*}\left(\hat{\lambda} + \widetilde{S}_1(1-a-\hat{\lambda})\right), \quad I_{x,1}^* = \frac{\beta(1-\lambda_I)}{K^*}\left((1-a-\hat{\lambda}) + \widetilde{S}_1\hat{\lambda}\right)$$

3. Investments in the green technology:

$$I_g = \frac{\beta a}{K}\left(\widetilde{S}_1\lambda_g + 1 - \lambda_g\right), \quad I_g^* = \frac{\beta a}{K^*}\left(\lambda_g + \widetilde{S}_1(1-\lambda_g)\right),$$

where

$$\begin{aligned} K &= 1 - \lambda + \beta\lambda_I(1-a-\hat{\lambda}) + \beta(1-\lambda_I)\hat{\lambda} + \beta a(1-\lambda_g) + \left[\lambda + \beta\lambda_I\hat{\lambda} + \beta(1-\lambda_I)(1-a-\hat{\lambda}) + \beta a\lambda_g\right]\widetilde{S}_1, \\ K^* &= \lambda + \beta\lambda_I\hat{\lambda} + \beta(1-\lambda_I)(1-a-\hat{\lambda}) + \beta a\lambda_g + \left[1 - \lambda + \beta\lambda_I(1-a-\hat{\lambda}) + \beta(1-\lambda_I)\hat{\lambda} + \beta a(1-\lambda_g)\right]\widetilde{S}_1. \end{aligned}$$

Note that if $\widetilde{S}_1 = 1$, $K = K^* = (1+\beta)$.

Log-linearizing the optimal allocations around $\overline{\widetilde{s}_1} = \log\overline{\widetilde{S}_1} = 0$, we obtain:

$$\begin{aligned} \log X_1 &\approx \log\frac{\lambda}{1+\beta} + \lambda_x^s \cdot \widetilde{s}_1, & \log X_1^* &\approx \log\frac{1-\lambda}{1+\beta} + \lambda_{x^*}^s \cdot \widetilde{s}_1, \\ \log Y_1 &\approx \log\frac{1-\lambda}{1+\beta} - \lambda_{x^*}^s\widetilde{s}_1, & \log Y_1^* &\approx \log\frac{\lambda}{1+\beta} - \lambda_x^s\widetilde{s}_1, \\ \log I_{x,1} &\approx \log\frac{\beta\lambda_I(1-a)}{1+\beta} + \lambda_{I_x}^s \cdot \widetilde{s}_1, & \log I_{y,1} &\approx \log\frac{\beta(1-\lambda_I)(1-a)}{1+\beta} + \lambda_{I_y}^s \cdot \widetilde{s}_1, \\ \log I_{x,1}^* &\approx \log\frac{\beta(1-\lambda_I)(1-a)}{1+\beta} - \lambda_{I_y}^s\widetilde{s}_1, & \log I_{y,1}^* &\approx \log\frac{\beta\lambda_I(1-a)}{1+\beta} - \lambda_{I_x}^s\widetilde{s}_1, \\ \log I_g &\approx \log\frac{\beta a}{1+\beta} + \lambda_{I_g}^s \cdot \widetilde{s}_1, & \log I_g^* &\approx \log\frac{\beta a}{1+\beta} - \lambda_{I_g}^s\widetilde{s}_1, \end{aligned} \tag{C.11}$$

where

$$\lambda_x^s = \frac{1-\lambda+\beta\lambda_I(1-a-\hat{\lambda})+\beta(1-\lambda_I)\hat{\lambda}+\beta a(1-\lambda_g)}{1+\beta}, \quad \lambda_{x^*}^s = \lambda_x^s - 1 \tag{C.12}$$

$$\lambda_{I_x}^s = \frac{a(\lambda-\lambda_g)}{1-a} + \frac{\beta(1-\lambda_I)\left(2\hat{\lambda}-(1-a)\right)}{1+\beta}, \quad \lambda_{I_y}^s = \lambda_{I_x}^s - \frac{2\hat{\lambda}-1+a}{1-a}, \quad \lambda_{I_g}^s = \lambda_{I_x}^s + \frac{\lambda_g-\lambda}{1-a}.$$

Signs of the slopes of the log-linearized solution. We can characterize the slopes of the log-linearized solutions in (C.12). In what follows, we retain the parametric restrictions of Assumption C1.

1. Given that $\lambda, \lambda_g < 1$ and $\hat{\lambda} < 1-a$, we can easily verify that $\lambda_x^s > 0$.

2. Consider the inequality:

   $$1-\lambda+\beta\lambda_I(1-a-\hat{\lambda})+\beta(1-\lambda_I)\hat{\lambda}+\beta a(1-\lambda_g) < 1+\beta\lambda_I(1-a)+\beta(1-\lambda_I)(1-a)+\beta a = 1+\beta.$$

   From this, we conclude that $\lambda_x^s < 1$, and thus $\lambda_{x^*}^s = \lambda_x^s - 1 < 0$.

3. Since

   $$\lambda_{I_x}^s = \frac{a(\lambda-\lambda_g)}{1-a} + \frac{\beta(1-\lambda_I)\left(2\hat{\lambda}-(1-a)\right)}{1+\beta},$$

   it follows that if $\lambda > \lambda_g$ and $\hat{\lambda} > \frac{1-a}{2}$, then $\lambda_{I_x}^s > 0$. Otherwise, $\lambda_{I_x}^s$ can be negative.

4. Note that

   $$\begin{aligned}\lambda_{I_y}^s &= \frac{(1+\beta)a(\lambda-\lambda_g)+(1+\beta a)(1-a-2\hat{\lambda})+\beta\lambda_I(1-a)(1-a-2\hat{\lambda})}{(1+\beta)(1-a)} \\ &= \frac{a(\lambda-\lambda_g)+1-a-2\hat{\lambda}+\beta\lambda_I(1-a)(1-a-2\hat{\lambda})+\beta a(1-a-2\hat{\lambda}+\lambda-\lambda_g)}{(1+\beta)(1-a)} \\ &= \frac{(1-\lambda)(1-a)-\hat{\lambda}+\beta\lambda_I(1-a)(1-a-2\hat{\lambda})+\beta a\left((1-\lambda_g)(1-a)-\hat{\lambda}\right)}{(1+\beta)(1-a)}.\end{aligned}$$

   Since $(1-\lambda)(1-a) < \frac{1-a}{2}$, $(1-\lambda_g)(1-a) < \frac{1-a}{2}$, and $\hat{\lambda} > \frac{1-a}{2}$, the numerator is negative. Therefore, $\lambda_{I_y}^s < 0$.

5. Finally, since

   $$\lambda_{I_g}^s = \lambda_g - \lambda + \frac{\beta(1-\lambda_I)\left(2\hat{\lambda}-(1-a)\right)}{1+\beta},$$

   and $\hat{\lambda} > \frac{1-a}{2}$, we have $\lambda_{I_g}^s > 0$ when $\lambda < \lambda_g$. Otherwise, $\lambda_{I_g}^s$ may be negative.

TABLE C.1. SIGNS OF THE SLOPES OF THE LOG-LINEARIZED SOLUTION

	λ^s_x	$\lambda^s_{x^*}$	$\lambda^s_{I_x}$	$\lambda^s_{I_y}$	$\lambda^s_{I_g}$
$\lambda > \lambda_g$	+	−	+	−	Undetermined
$\lambda < \lambda_g$	+	−	Undetermined	−	+

Notes: The table reports the signs of the slopes of the log-linearized solution of the model reported in (C.12). These sign conclusions hold based on the domain restrictions assumed in Assumption C1.

Table C.1 summarizes the signs of the slopes of the log-linearized allocations in (C.12).

Equilibrium utilities. Starting from the time $t = 1$ utilities in (C.1), we substitute the log-linearized allocations from (C.11), along with the definitions of $\log D_2$ and $\log D_2^*$ in (C.6), and the definitions of B and B^* in (C.2), to obtain:

$$\begin{aligned} u_1 &= const + \lambda_u^\theta \theta + b\lambda_u^g g + \lambda_u^s \widetilde{s}_1 = const + \left(\lambda_u^\theta + \lambda_u^s \lambda_s^\theta\right)\theta + \left(b\lambda_u^g + \lambda_u^s \lambda_s^g\right) g \\ u_1^* &= const - \lambda_u^\theta \theta + \lambda_u^g g - \lambda_u^s \widetilde{s}_1 = const - \left(\lambda_u^\theta + \lambda_u^s \lambda_s^\theta\right)\theta - \left(-\lambda_u^g + \lambda_u^s \lambda_s^g\right) g \end{aligned} \tag{C.13}$$

where the second equality follows from the linearity of $\widetilde{s}_1$ in the two shocks (see C.4) and where

$$\begin{aligned} \lambda_u^\theta &= \tilde{\beta}\left(2\hat{\lambda} - (1-a)\right), \quad \lambda_u^g = -\beta(1-\beta)a, \\ \lambda_u^s &= (1-\beta)\left(\lambda\lambda_x^s - (1-\lambda)\lambda_{x^*}^s\right) + \tilde{\beta}\left(2\lambda(1-\lambda) + (2\hat{\lambda} - 1 + a)\left(\lambda_I \lambda_{I_x}^s - (1-\lambda_I)\lambda_{I_y}^s\right) + a(2\lambda_g - 1)\lambda_{I_g}^s\right). \end{aligned} \tag{C.14}$$

and $\tilde{\beta} = \beta(1-\beta)$.

Sensitivity of the Pareto weights to the shocks. Recall from equation (C.3) that the log-ratio of the Pareto weights at date $t = 1$ is equal to $\widetilde{s}_1 = (u_1 - u_1^*)(1-\gamma)$. Since utilities are linear functions of the shocks θ and g (see (C.13)), it follows that $\widetilde{s}_1$ is also linear in the shocks:

$$\widetilde{s}_1 = \bar{s} + \lambda_s^\theta \cdot \theta + \lambda_s^g \cdot g, \tag{C.15}$$

where

$$\lambda_s^\theta = 2(1-\gamma)\left(\lambda_u^\theta + \lambda_u^s \lambda_s^\theta\right), \quad \lambda_s^g = (1-\gamma)\left((b-1)\lambda_u^g + 2\lambda_u^s \lambda_s^g\right),$$

where λ_u^g, λ_u^s, and λ_s^g are defined in (C.14). Solving these equations yields:

$$\lambda_s^\theta = \frac{2(1-\gamma)\lambda_u^\theta}{1+2(\gamma-1)\lambda_u^s}, \qquad \lambda_s^g = \frac{(1-\gamma)(b-1)\lambda_u^g}{1+2(\gamma-1)\lambda_u^s}. \tag{C.16}$$

Next we examine how the ratio of the pseudo Pareto weights responds to different shocks.

Lemma 1. *Under Assumption C1, $\lambda_u^s > 0$. In addition, when $\gamma > 1$ we have: (i) $\lambda_s^\theta < 0$, and (ii) $\lambda_s^g > 0$ (< 0) if $b > 1$ (< 1).*

Proof. First, we prove that the coefficient λ_u^s defined in (C.14) is always strictly larger than zero. We notice the following:

1. When $\lambda > \lambda_g$, we conclude that $\lambda\lambda_x^s - (1-\lambda)\lambda_{x^*}^s > 0$ and $\lambda_I\lambda_{I_x}^s - (1-\lambda_I)\lambda_{I_y}^s > 0$, based on the characterization of the signs of the slopes of the log-linear solution for the allocations in Table C.1. We now need to verify that the negative contribution associated with $\lambda_{I_g}^s$ does not outweigh the positive terms. From the expression $(1-\beta)\left(\lambda\lambda_x^s - (1-\lambda)\lambda_{x^*}^s\right)$, we can extract a strictly positive term $(1-\beta)(1-\lambda) > 0$ (since $\lambda_{x^*}^s = \lambda_x^s - 1$) and retain the remaining positive part. The negative component coming from $\lambda_{I_g}^s$ is given by $(1-\beta)\beta a(2\lambda_g - 1)(\lambda_g - \lambda)$. Thus, we need to verify that

$$(1-\beta)(1-\lambda) + (1-\beta)\beta a(2\lambda_g - 1)(\lambda_g - \lambda) > 0,$$

   or, equivalently,

$$1 - \lambda + \beta a(2\lambda_g - 1)(\lambda_g - \lambda) > 0$$

   under the parameter restrictions in Assumption C1. Note that $\hat{\lambda} < 1 - a$ also implies:

$$\lambda < 1 - a + a\lambda_g.$$

   Then,

$$\begin{aligned} 1 - \lambda + \beta a(2\lambda_g - 1)(\lambda_g - \lambda) &> 1 - (1 - a + a\lambda_g) + \beta a(2\lambda_g - 1)\left(\lambda_g - (1 - a + a\lambda_g)\right) \\ &= a(1-\lambda_g) + \beta a(2\lambda_g - 1)(1-a)(\lambda_g - 1) \\ &= a(1-\lambda_g)\left(1 - \beta(2\lambda_g - 1)(1-a)\right) \\ &> 0, \end{aligned}$$

   where the final inequality holds because $\beta < 1$, $2\lambda_g - 1 < 1$, and $1 - a < 1$.

2. When $\lambda < \lambda_g$, the only negative component in λ_u^s is associated with $\lambda_{I_x}^s$, based on the

sign characterization in Table C.1. The negative term is given by

$$(1-\beta)\beta(2\hat{\lambda}-1+a)\lambda_I\frac{a}{1-a}(\lambda-\lambda_g).$$

As before, given that $(1-\beta)(1-\lambda)>0$, we need to verify that

$$1-\lambda>\beta(2\hat{\lambda}-1+a)\lambda_I\frac{a}{1-a}(\lambda_g-\lambda).$$

Note that

$$\frac{2\hat{\lambda}-1+a}{1-a}=\frac{2\hat{\lambda}}{1-a}-1<1,$$

since $\hat{\lambda}<1-a$. It follows that

$$\beta(2\hat{\lambda}-1+a)\lambda_I\frac{a}{1-a}(\lambda_g-\lambda)<\beta a\lambda_I(\lambda_g-\lambda)<\lambda_g-\lambda<1-\lambda.$$

The above derivations prove that $\lambda_s^u>0$. The characterization of the signs of λ_u^θ and λ_u^g in (C.14) is straightforward:

$$\lambda_u^\theta=\beta(1-\beta)\left(2\hat{\lambda}-(1-a)\right)>0,\quad \lambda_u^g=-\beta(1-\beta)a<0.$$

We conclude that $\lambda_s^\theta<0$ when $\gamma>1$. In addition, when $b>1$ (<1), $\lambda_s^g>0$ (<0). □

C.2.1 Exchange rates

Since markets are complete, the growth rate of the exchange rate equals the ratio of the stochastic discount factors (SDFs). We can characterize this ratio using the equilibrium condition for the ratio of Pareto weights:

$$\widetilde{S}_1=\widetilde{S}_0\frac{M_1}{M_1^*}\frac{e^{\Delta c_1}}{e^{\Delta c_1^*}},$$

where M_1 and M_1^* denote the SDFs for the home and foreign countries, respectively. Taking logarithms yields:

$$\widetilde{s}_1=\widetilde{s}_0+m_1-m_1^*+\Delta c_1-\Delta c_1^*.$$

Note that $\Delta e_1=m_1-m_1^*$, where Δe_1 is the log change in the real exchange rate (measured as the amount of foreign currency per unit of domestic currency). Given that $\widetilde{S}_0$, c_0, and c_0^* are

constants that do not depend on the shocks, we have:

$$\begin{aligned}\Delta e_1 &= \text{const} + \widetilde{s}_1 - c_1 + c_1^* \\ &= \text{const} + \widetilde{s}_1 - (\lambda \log X_1 + (1-\lambda)\log Y_1) + (\lambda \log Y_1^* + (1-\lambda)\log X_1^*) \\ &= \text{const} + \widetilde{s}_1 - (\lambda\lambda_x^s - (1-\lambda)\lambda_{x^*}^s)\,\widetilde{s}_1 + (-\lambda\lambda_x^s + (1-\lambda)\lambda_{x^*}^s)\,\widetilde{s}_1 \\ &= \text{const} + \lambda_e^s \cdot \widetilde{s}_1,\end{aligned}$$

where

$$\lambda_e^s = 1 - 2\left(\lambda\lambda_x^s - (1-\lambda)\lambda_{x^*}^s\right). \tag{C.17}$$

Thus, there is a one-to-one mapping between the pseudo-Pareto weight $\widetilde{S}_1$ and changes in the real exchange rate. The nature of this relationship depends on the sign of λ_e^s. The following proposition establishes that $\lambda_e^s > 0$ under Assumption C1.

Proposition 1. *Let $\gamma > 1$, when $b > 1$ ($b < 1$), a global climate news shock $g > 0$ causes an appreciation of home (foreign) real exchange rate.*

Proof. We need to characterize the sign of the composite coefficient λ_e^s in equation (C.17). Using $\lambda_{x^*}^s = \lambda_x^s - 1$ (see (C.12)) in the definition of λ_e^s, we need to show that

$$\lambda_e^s = 1 - 2(\lambda\lambda_x^s - (1-\lambda)(\lambda_x^s - 1)) = 1 - 2((2\lambda - 1)\lambda_x^s + (1-\lambda)) > 0$$

which is equivalent to $(2\lambda - 1)\lambda_x^s < \lambda - \frac{1}{2}$ or $\lambda_x^s < \frac{1}{2}$. By using the expression for λ_x^s in (C.12), we obtain:

$$1 - \lambda + \beta\lambda_I(1 - a - \hat{\lambda}) + \beta(1-\lambda_I)\hat{\lambda} + \beta a(1-\lambda_g) < \frac{1+\beta}{2}.$$

Note that

$$\beta\lambda_I(1 - a - \hat{\lambda}) + \beta(1-\lambda_I)\hat{\lambda} = \beta\left(\lambda_I(1 - a - 2\hat{\lambda}) + \hat{\lambda}\right).$$

Given $1 - a - 2\hat{\lambda} < 0$ (Assumption C1) and $\lambda_I > 0$, then $\beta\lambda_I(1 - a - \hat{\lambda}) + \beta(1-\lambda_I)\hat{\lambda} < \beta\hat{\lambda}$. Then it is sufficient to prove that:

$$1 - \lambda + \beta\hat{\lambda} + \beta a(1-\lambda_g) < \frac{1+\beta}{2}.$$

Since $\hat{\lambda} = \lambda - a\lambda_g$, the left hand side of the above expression becomes

$$1 - \lambda + \beta\lambda + \beta a(1 - 2\lambda_g) < 1 - \lambda + \beta\lambda.$$

Since $1-2\lambda_g<0$, a sufficient condition is then $1-\lambda+\beta\lambda<\frac{1+\beta}{2}$. After rearranging, we need $\beta\left(\lambda-\frac{1}{2}\right)<\lambda-\frac{1}{2}$. This condition holds because $\lambda-\frac{1}{2}>0$ and $\beta<1$. □

C.2.2 Cross section of returns

We characterize the returns to both brown and green capital in the home country. We choose the home country because its exposure to climate news, b, can take values other than 1. In this two-period model, we focus on investment returns at $t=1$ and derive their exposure coefficients with respect to our exogenous shocks. In particular, we define the returns as follows

$$R_{i,1|0}=\frac{Q_{i,1}}{Q_{i,0}} \tag{C.18}$$

where $Q_{i,t}$ denotes the time-t ex-dividend value of the marginal cash-flows paid out by investment in the final period of the model. We denote brown and green investment by $i\in\{b,g\}$, respectively.

In our empirical investigation, we focus on the 'betas' of these returns with respect to climate news shocks. Since all time-0 variables are pre-determined in our model, both returns react to shocks through their numerator, that is, the revised valuation of future cash-flows, $Q_{i,1}$. In order to get predictions on the betas of these returns, all we need to do is to log-linearize their numerator. All other terms would be comprised in the constant of our approximation and would determine the equilibrium average risk premium. In practice, $Q_{i,1}$ is simply the marginal Tobin's Q assessed at the equilibrium. Note that because of our Cobb-Douglas aggregators, our model features diminishing marginal returns from investment, or, equivalently, convex adjustment costs and time-varying Tobin's Q.

Brown investment returns. Since in this model $Q_b:=\frac{1}{B_{I_{x,1}}}=\frac{1}{\lambda_I}\frac{I_{x,1}}{B}$, the log-linear brown return is:

$$r_{b,1}=constant+\log I_{x,1}-\log B=constant+(1-\lambda_I)\left(\log I_{x,1}-\log I^*_{x,1}\right). \tag{C.19}$$

Green investment returns. Define $G:=I_g^{\lambda_g}I_g^{*1-\lambda_g}$, the implied Tobin's Q for domestic investment in X units is: $Q_g:=\frac{1}{\partial G/\partial I_g}=\frac{1}{\lambda_g}\frac{I_g}{G_g}$. The log-linear return of green investment is

$$r_{g,1}=costant+\log I_g-\log G=constant+(1-\lambda_g)\left(\log I_g-\log I^*_g\right) \tag{C.20}$$

The brown-minus-green return. We examine the heterogeneous exposure of brown and green returns to a global climate shock by constructing the brown-minus-green investment return. Given Equations C.19 and C.20,

$$r_{b,1} - r_{g,1} = constant + (1-\lambda_I)\left(\log I_{x,1} - \log I^*_{x,1}\right) - (1-\lambda_g)\left(\log I_g - \log I^*_g\right)$$

Utilizing the log-linearized formulas for investments, we get

$$r_{b,1} - r_{g,1} = constant + \left[\underbrace{(1-\lambda_I)\left(\lambda^s_{I_x} + \lambda^s_{I_y}\right) - 2(1-\lambda_g)\lambda^s_{I_g}}_{\lambda^s_{r_b - r_g}}\right]\widetilde{s}_1$$

Hence the green-minus-brown return adjustments are solely driven by the pseudo-Pareto weight $\widetilde{s}_1$.

Lemma 2. *Given Assumption C1, if $\lambda_g \geq \lambda$, then $\lambda^s_{r_b - r_g} < 0$, that is, the brown-minus-green return decreases when the pseudo-Pareto weight increases.*

Proof. Given the formula for $\lambda^s_{I_x}$, $\lambda^s_{I_y}$, and $\lambda^s_{I_g}$, we obtain

$$\begin{aligned}
\lambda^s_{r_b - r_g} &= (1-\lambda_I)\left(\lambda^s_{I_x} + \lambda^s_{I_y}\right) - 2(1-\lambda_g)\lambda^s_{I_g} \\
&= (1-\lambda_I)\left(\frac{2a(\lambda-\lambda_g)}{1-a} + \frac{\beta(1-\lambda_I)(2\hat{\lambda}-1+a)(1-a) + (1+a\beta+\beta\lambda_I(1-a))(1-a-2\hat{\lambda})}{(1+\beta)(1-a)}\right) \\
&\quad -2(1-\lambda_g)\left(\lambda_g - \lambda + \frac{\beta(1-\lambda_I)(2\hat{\lambda}-1+a)}{1+\beta}\right) \\
&= \underbrace{2(\lambda-\lambda_g)\left(\frac{a}{1-a}(1-\lambda_I) + 1 - \lambda_g\right)}_{\leq 0} + \underbrace{(1-\lambda_I)\frac{(2\hat{\lambda}-1+a)\left(\beta(1-2\lambda_I)(1-a) - 1 - a\beta\right)}{(1+\beta)(1-a)}}_{<0} \\
&\quad \underbrace{-2(1-\lambda_g)\frac{\beta(1-\lambda_I)(2\hat{\lambda}-1+a)}{1+\beta}}_{>0} \\
&< 0
\end{aligned}$$

The signs of above terms hold under the Assumption C1 and with $\lambda_g \geq \lambda$.

□

Note that the pseudo-Pareto weight depends on the shocks with the following linear func-

tional form

$$\widetilde{s}_1 = \lambda_s^\theta \theta + \lambda_s^g g$$

where the coefficients λ_s^θ and λ_s^g are defined in (C.16). Therefore,

$$r_{b,1} - r_{g,1} = constant + \lambda^s_{r_x - r_g} \lambda_s^\theta \theta + \lambda^s_{r_x - r_g} \lambda_s^g g + \lambda^s_{r_x - r_g} \lambda_s^z z \tag{C.21}$$

Given our results in Lemma 1, we obtain the following proposition:

Proposition 2. *If $b > 1$, the brown-minus-green investment return in the home country depreciates when there is a positive global climate shock $g > 0$. In addition, the effect is stronger with a higher b*

Proof. Note that $\lambda^s_{r_b - r_g} < 0$ and $\lambda_s^g > 0$ when $b > 1$. In addition, λ_s^g is increasing with country exposure b. □

C.2.3 Net exports

Using the definition of net export of consumption, we obtain what follows:

$$\begin{aligned} \frac{NX_1^C}{X_1} &= \frac{X_1^*}{X_1} - \left(\frac{1-\lambda}{\lambda}\frac{X_1}{Y_1}\right)\frac{Y_1}{X_1} = \frac{1-\lambda}{\lambda}\left(\frac{1}{\widetilde{S}_1} - 1\right) \\ &= -\left(\frac{1-\lambda}{\lambda}\right)\left[\frac{(\exp\{\tilde{s}_1\} - 1)}{1 + (\exp\{\tilde{s}_1\} - 1)}\right]. \end{aligned} \tag{C.22}$$

Similarly, using the definition of net export of investments, we get:

$$\begin{aligned} \frac{NX_1^I}{I_x} &= \frac{I_y}{I_x} - \left(\frac{1-\lambda_I}{\lambda_I}\frac{I_x}{I_x^*}\right)\frac{I_x^*}{I_x} = \frac{1-\lambda_I}{\lambda_I}\left(\frac{\widetilde{S}_1 + \hat{\kappa}}{\hat{\kappa}\widetilde{S}_1 + 1} - 1\right) \\ &= -\left(\frac{1-\lambda_I}{\lambda_I}\right)\left[\frac{(\hat{\kappa} - 1)\cdot(\exp\{\tilde{s}_1\} - 1)}{1 + \hat{\kappa}\cdot(\exp\{\tilde{s}_1\} - 1)}\right], \end{aligned} \tag{C.23}$$

where $\hat{\kappa} = \frac{\hat{\lambda}}{1-a-\hat{\lambda}} = \frac{\lambda - a\lambda_g}{1-\lambda-a(1-\lambda_g)} > 1$. We can characterize the response of net exports to the shocks in the following proposition.

Proposition 3. *Let $\gamma > 1$, when $b > 1$, a global climate news shock $g > 0$ decreases total net exports in the home country, implying that there is a reallocation of resources toward the country that ex-ante hedges the most.*

Proof. Both net export functions in (C.22) and (C.23) are decreasing in $(\exp\{\tilde{s}_1\} - 1)$. Combining this observation with Lemma 1 concludes the proof. □

These derivations set the stage for our empirical analysis. For the home country, net exports of consumption goods are given by

$$\frac{NX_1^C}{X_1} = \frac{1-\lambda}{\lambda}\left(\frac{1}{\widetilde{S}_1} - 1\right) = \text{const} - \frac{1-\lambda}{\lambda} e^{-\bar{s}_1}\widetilde{S}_1.$$

By symmetry, net exports of the foreign country are

$$\frac{NX_1^{C*}}{Y_1^*} = \frac{1-\lambda}{\lambda}\left(\widetilde{S}_1 - 1\right) = \text{const} + \frac{1-\lambda}{\lambda} e^{\bar{s}_1}\widetilde{S}_1.$$

Thus,

$$\frac{NX_1^C}{X_1} - \frac{NX_1^{C*}}{Y_1^*} = \text{const} - \frac{1-\lambda}{\lambda}(e^{\bar{s}_1} + e^{-\bar{s}_1})\widetilde{S}_1.$$

Given that

$$\widetilde{s}_1 = \bar{s}_1 + \lambda_s^\theta \theta + \lambda_s^g g,$$

it follows that

$$\frac{NX_1^C}{X_1} - \frac{NX_1^{C*}}{Y_1^*} = \text{const} + \beta_\theta^{NX} \cdot 2\theta + \beta_g^{NX}(b-1)g,$$

where, according to Lemma 1,

$$\begin{aligned} \beta_\theta^{NX} &= -\frac{1}{2}\frac{1-\lambda}{\lambda}(e^{\bar{s}_1} + e^{-\bar{s}_1})\lambda_s^\theta > 0, \\ \beta_g^{NX} &= -\frac{1}{2}\frac{1-\lambda}{\lambda}(e^{\bar{s}_1} + e^{-\bar{s}_1})\frac{\lambda_s^g}{b-1} < 0. \end{aligned}$$

Similarly, the same relationship holds for net exports of investment goods. As a result, total net export differentials are positively related to a positive productivity shock ($\theta > 0$) and negatively related to a global climate sentiment shock ($g > 0$), provided that $b > 1$.

C.2.4 Additional Model Results

Stochastic discount factor. Let's examine how the stochastic discount factor responds to different shocks. Note that for the home country, the SDF at time 1 is given by

$$M_1 = \frac{\partial u_0 / \partial C_1}{\partial u_0 / \partial C_0}$$

where u_0 is the utility at time 0,

$$u_0 = (1-\beta)\log C_0 D_0^{-\alpha} + \frac{\beta}{1-\gamma}\log E_0\left[\exp\left\{u_1(1-\gamma)\right\}\right]$$

As a result, we get:

$$M_1 = \beta \frac{C_0}{C_1} \frac{\exp\left(u_1(1-\gamma)\right)}{E_0\left[\exp\left(u_1(1-\gamma)\right)\right]},$$

and in log-units:

$$m_1 = \log(\beta) + \log\left(C_0\right) - \log\left(C_1\right) + (1-\gamma)u_1 - \log E_0\left[\exp\left(u_1(1-\gamma)\right)\right].$$

Substituting the expressions of $\log C_1$ and u_1,

$$m_1 = const - (\lambda\lambda_x^s - (1-\lambda)\lambda_{x^*}^s)\widetilde{s}_1 + (1-\gamma)(\lambda_\theta\theta + \lambda_z z + \lambda_g g),$$

where all time-0 terms end up in the constant. In addition, note that

$$(1-\gamma)\lambda_\theta = \frac{1}{2}\lambda_s^\theta, \quad (1-\gamma)\lambda_z = \frac{1}{2}\lambda_s^z,$$

$$(1-\gamma)\lambda_g = (1-\gamma)\left(b\lambda_u^g + \lambda_u^s\lambda_s^g\right) = \underbrace{(1-\gamma)\left(\frac{b-1}{2}\lambda_u^g + \lambda_u^s\lambda_s^g\right)}_{\frac{1}{2}\lambda_s^g} + (1-\gamma)\frac{b+1}{2}\lambda_u^g.$$

Thus

$$m_1 = const + \underbrace{\left(\frac{1}{2} - (\lambda\lambda_x^s - (1-\lambda)\lambda_{x^*}^s)\right)}_{\frac{1}{2}\lambda_e^s}\widetilde{s}_1 + \frac{1}{2}(1-\gamma)(1+b)\lambda_u^g g.$$

Similarly, the SDF for the foreign country is

$$m_1^* = const - \frac{1}{2}\lambda_e^s\widetilde{s}_1 + \frac{1}{2}(1-\gamma)(1+b)\lambda_u^g g$$

The expressions of two SDFs also verifies that

$$\Delta e_1 = m_1 - m_1^* = const + \lambda_e^s\widetilde{s}_1$$

We have shown that $\lambda_e^s > 0$ in Proposition 1. In addition, $\lambda_u^g = -\beta(1-\beta)a < 0$. Hence if we hold the Pareto weight constant, a global climate shock increases the SDFs for both countries.

Proposition 4. *Holding g constant, there is a one-to-one mapping between the SDF and the pseudo-Pareto weight $\widetilde{S}_1$. An increase in $\widetilde{S}_1$ corresponds to an increase in m_1 and a decrease in m_1^*).*

Thus both productivity shock θ has an unambiguous effect on the SDF of the two countries. The effect of the global climate shock g is unambiguous conditional on the following parameter

restrictions.

Proposition 5. *Let $\gamma > 1$, when $b > 1$ ($b < 1$), a positive global climate news shock increases (decreases) the SDF of the home country relative to the foreign country.*

C.3. A Simplified Setting with $\lambda = \lambda_I = \lambda_g$

In this section, we assume that all Cobb-Douglas parameters are identical: $\lambda = \lambda_g = \lambda_I$. More precisely, we impose the following restrictions on the domain of the model's parameters.

Assumption S1. *We impose the following parametric restrictions: $\lambda = \lambda_g = \lambda_I$, $a \in (0,1)$, $b > 1$, $\gamma > 1$, $\lambda \in (1/2, 1)$ and $\beta \in (0,1)$.*

It is straightforward to show that the equilibrium coefficients that govern the allocation of consumption and investment goods simplify to:

$$\begin{aligned} &\hat{\lambda} = \lambda(1-a), \quad \lambda_{Ix}^S = \frac{\beta}{1+\beta}(1-\lambda)(2\lambda-1)(1-a), \quad \lambda_{Iy}^S = (1-2\lambda) + \lambda_{Ix}^S, \\ &\lambda_x^S = (1-\lambda) + \lambda_{Ix}^S, \quad \lambda_{x^*}^S = -\lambda + \lambda_{Ix}^S, \quad \lambda_{Ig}^S = \lambda_{Ix}^S. \end{aligned} \tag{C.24}$$

Similarly, the equilibrium coefficients that govern the response of the utility functions to the fundamental shocks simplify to:

$$\begin{aligned} &\lambda_u^\theta = \beta(1-\beta)(1-a)(2\lambda-1), \quad \lambda_u^g = -\beta(1-\beta)a, \quad \lambda_u^z = -\beta(1-\beta)a(2\lambda-1) \\ &\lambda_\theta = \frac{\lambda_u^\theta}{1+2(\gamma-1)\lambda_u^s}, \quad \lambda_g = \frac{b + 2b(\gamma-1)\lambda_u^s - (\gamma-1)(b-1)\lambda_u^s}{1+2(\gamma-1)\lambda_u^s} \cdot \lambda_u^g. \end{aligned} \tag{C.25}$$

The parameter $\hat{\kappa}$ that governs the sensitivity of the net exports of investment goods simplifies to $\hat{\kappa} = \frac{\lambda}{1-\lambda}$.

The next lemma mirrors Lemma 1 in the general setting.

Lemma S1. Ratio of Pareto weights *The log-ratio of the Pareto weights at time $t = 1$ is equal to:*

$$\tilde{s}_1 \quad = \quad \bar{s} + \tilde{\beta} \cdot (\gamma - 1) \cdot \left[\left(\frac{(b-1)a}{1+2(\gamma-1)\lambda_u^s} \right) \cdot g - \left(\frac{(1-a)(2\lambda-1)}{1+2(\gamma-1)\lambda_u^s} \right) \cdot 2\theta \right], \tag{C.26}$$

where $\tilde{\beta} = \beta(1-\beta)$*, and*

$$\begin{aligned}\lambda_{Ix}^S &= \frac{\beta}{1+\beta}(1-\lambda)(2\lambda-1)(1-a) > 0\\ \lambda_u^s &= (1-\beta)\left\{(1-\lambda)\left[2\lambda(1+\beta)+\beta(2\lambda-1)^2(1-a)\right]+(2\lambda-1)\left[1+a\beta+(1-a)(2\lambda-1)\beta\right]\lambda_{Ix}^S\right\} > 0.\end{aligned}$$

Then the log-ratio of the Pareto weights $\tilde{s}_1$ *increases in response to a positive sentiment shock* ($g > 0$) *and it decreases in response to a positive productivity shock* ($\theta > 0$)*.*

Proof. Recall that $\tilde{s}_1 = (u_1 - u_1^*)(1-\gamma)$. It follows that the loading on the g shock in $\tilde{s}_1$ is:

$$(1-\gamma)\left[(b\lambda_u^g + \lambda_u^s\lambda_s^g) + (-\lambda_u^g + \lambda_u^s\lambda_s^g)\right] = \beta(1-\beta)\cdot\frac{(\gamma-1)(b-1)a}{1+2(\gamma-1)\lambda_u^s}$$

and that the loading on the θ shock in $\tilde{s}_1$ is

$$2\lambda_\theta(1-\gamma) = 2\beta(1-\beta)\cdot\frac{(\gamma-1)(a-1)(2\lambda-1)}{1+2(\gamma-1)\lambda_u^s},$$

where we used the expression for λ_u^g, λ_s^g, λ_θ from the system of equations (C.25). The positivity of λ_{Ix}^S and λ_u^s as well as of the loadings on g and θ follows immediately from the domain restrictions on a, b, γ, and λ. □

The next proposition mirrors Proposition 1 in the general setting.

Proposition S1. Exchange rates *The log-growth rate of the exchange rate at date* $t = 1$ *is equal to:*

$$\Delta e_1 = \overline{\Delta e} + \lambda_e^s \cdot \tilde{s}_1, \tag{C.27}$$

where

$$\lambda_e^s = (2\lambda-1)^2\cdot\left[1 - 2\frac{\beta}{1+\beta}(1-\lambda)(1-a)\right] > 0. \tag{C.28}$$

It follows that the exchange rate appreciates in response to a positive sentiment shock ($g > 0$) *and it depreciates in response to a positive productivity shock* ($\theta > 0$)*.*

Proof. The loading of the exchange rate on the ratio of Pareto weights is

$$\lambda_e^s = 1 - 2\left[\lambda\lambda_x^s - (1-\lambda)\lambda_{x*}^s\right] = 1 - 2\left[\lambda\lambda_x^s - (1-\lambda)\left(\lambda_x^s - 1\right)\right] = (2\lambda-1)\left(1-2\lambda_x^s\right),$$

where the second equality follows from $\lambda^s_{x*} = \lambda^s_x - 1$. Using the equation for λ^s_x first and for λ^s_{Ix} second from system (C.24), we obtain

$$\lambda^s_e = (2\lambda - 1)\left(2\lambda - 1 - 2\lambda^s_{Ix}\right) = (2\lambda - 1)^2 \cdot \left[1 - 2\frac{\beta}{1+\beta}(1-\lambda)(1-a)\right] > 0.$$

The term in bracket is positive because $2\frac{\beta}{1+\beta} < 1$ ($\beta \in (0,1)$) and $(1-\lambda)(1-a) < 1$ ($\lambda \in (1/2, 1)$ and $a \in (0,1)$), thus making the product of the two terms smaller than unity. Combining $\lambda^s_e > 0$ with Lemma S1 concludes the proof. □

The next proposition mirrors Proposition 2 in the general setting.

Proposition S2. Excess Returns *The log-return of brown stocks in excess of green stocks at date $t = 1$ is equal to:*

$$r_{b,1} - r_{g,1} \quad = \quad \bar{r} + \lambda^s_{r_b - r_g} \cdot \tilde{s}_1, \tag{C.29}$$

where

$$\lambda^s_{r_b - r_g} = (1-\lambda)(1-2\lambda) < 0.$$

It follows that the excess return declines in response to a positive sentiment shock ($g > 0$) and it increases in response to a positive productivity shock ($\theta > 0$).

Proof. Imposing $\lambda = \lambda_g = \lambda_I$ in the definition of $\lambda^s_{r_b - r_g}$ from the general model:

$$\begin{aligned}
\lambda^s_{r_b - r_g} &= (1-\lambda)\left(\lambda^s_{I_x} + \lambda^s_{I_y} - 2\lambda^s_{I_g}\right) \\
&= (1-\lambda)\left(\lambda^s_{I_x} + (1-2\lambda) + \lambda^s_{I_x} - 2\lambda^s_{I_x}\right) \\
&= (1-\lambda)(1-2\lambda) < 0,
\end{aligned}$$

which concludes the proof. □

The next proposition mirrors Proposition 3 in the general setting.

Proposition S3. Net Exports *Net exports of consumption and investment goods at time $t = 1$ are equal to:*

$$\frac{NX^C_1}{X_1} = -\left(\frac{1-\lambda}{\lambda}\right)\left[\frac{(\exp\{\tilde{s}_1\} - 1)}{1 + (\exp\{\tilde{s}_1\} - 1)}\right], \quad \frac{NX^I_1}{I_x} = -\left[\frac{(2\lambda - 1)(1-\lambda)}{\lambda}\right]\left[\frac{(\exp\{\tilde{s}_1\} - 1)}{1 + \lambda(\exp\{\tilde{s}_1\} - 1)}\right],$$

respectively. It follows that both net exports decline in response to a positive sentiment shock ($g > 0$) and increase in response to a positive productivity shock ($\theta > 0$).

Proof. The function for the net exports of consumption is identical as in the general model. The function for the net exports of investment obtains after observing that $\hat{\kappa} = \frac{\lambda}{1-\lambda}$. Both net export functions are decreasing in $(\exp\{\tilde{s}_1\} - 1)$. Combining this observation with Lemma S1 concludes the proof. □